Cotranslational transport of ABP140 mRNA to the distal pole of *S. cerevisiae*

Cornelia Kilchert and Anne Spang

Biozentrum, Universität Basel, Klingelbergstrasse 70, CH-4056 Basel, Switzerland

Corresponding author:

Anne Spang

Biozentrum

University of Basel

Klingelbergstrasse 70

CH-4056 Basel

Switzerland

Email: anne.spang@unibas.ch

Characters (including spaces): 50,786

Keywords: mRNA, localization, cotranslational

Subject Categories: RNA, Membranes & Transport

Abstract

In budding yeast, several mRNAs are selectively transported into the daughter cell in an actin-dependent manner by a specialized myosin system, the SHE machinery. With ABP140 mRNA, we now describe the first mRNA that is transported in the opposite direction and localizes to the distal pole of the mother cell, independent of the SHE machinery. Distal pole localization is not observed in mutants devoid of actin cables and can be disrupted by latrunculin A. Furthermore, localization of ABP140 mRNA requires the N-terminal actin-binding domain of Abp140p to be expressed. By replacing the N-terminal localization motif, ABP140 mRNA can be retargeted to different subcellular structures. In addition, accumulation of the mRNA at the distal pole can be prevented by disruption of polysomes. Using the MS2 system, the mRNA was found to associate with actin cables and to follow actin cable dynamics. We therefore propose a model of translational coupling, in which ABP140 mRNA is tethered to actin cables via its nascent protein product and is transported to the distal pole by actin retrograde flow.

Introduction

Many mRNAs are transported to defined subcellular localizations. Until recently, the prevailing view was that localized mRNAs are an exception to the rule, with mRNA transport affecting only selected transcripts (Holt and Bullock, 2009; Meignin and Davis, 2010). However, in a global analysis on mRNA localization in *Drosophila* oocytes and early embryos, a striking 70% of all transcripts displayed some type of subcellular localization. In this study, the authors distinguished dozens of distinct patterns (Lécuyer et al., 2007). Other genome-wide screens carried out in human cell lines identified mRNAs enriched on mitotic microtubules or in pseudopodia of migrating fibroblasts (Blower et al., 2007; Mili et al., 2008). Similarly, in yeast, several classes of localized transcripts have been described: mRNAs are specifically transported to the tip of the growing bud (Long et al., 1997; Takizawa et al., 1997; Shepard et al., 2003; Aronov et al., 2007), to the surface of mitochondria (Marc et al., 2002; Saint-Georges et al., 2008), or to peroxisomes (Zipor et al., 2009).

A growing amount of evidence suggests that the secretory pathway is involved in mRNA localization: Secretory mutants in *S. cerevisiae* show a defect in mRNA trafficking to the bud tip (Trautwein et al., 2004; Aronov and Gerst, 2004); in sensory neurons, the vesicular coat component Copb1 interacts with kappa opioid receptor mRNA and is required for its axonal transport (Bi et al., 2007); several proteins involved in vesicular transport were found to be enriched in polyadenylated mRNAs captured on oligo(dT) beads, among them components of the COPI coat (Tsvetanova et al., 2010). Finally, Sec27p, the β’ subunit of the COPI coat, was found to be associated with OXA1 mRNA (Slobodin and Gerst, 2010).

In our lab, we have been interested in the small GTPase Arf1p of *S. cerevisiae*, which is required for vesicle formation at the Golgi (for review, see D'Souza-Schorey and Chavrier, 2006). In several mutants of *ARF1*, ASH1 mRNA is not efficiently localized to the bud tip. Moreover, several mRNAs were found in a ribonucleoprotein complex present on Arf1p-

dependent COPI vesicles that mediate retrograde transport to the endoplasmic reticulum (ER) (Trautwein et al., 2004). In previous years, studies carried out in yeast and mammalian cells had revealed that many transcripts are enriched at the ER, including numerous mRNAs that encode cytosolic proteins and lack a signal sequence (Diehn et al., 2000; Lerner et al., 2003). To identify mRNAs that accumulate at the ER in an Arf1p-dependent manner, we analyzed the ER membrane-enriched 13,000 x g pellet of a temperature-sensitive *arf1* mutant by microarray and compared it to wild-type. One candidate that appeared in the screen was ABP140 mRNA. To our surprise, the mRNA localized to the distal pole of the mother cell in wild-type yeast. Here, we describe how ABP140 mRNA is transported to the distal pole of budding yeast. Localization of ABP140 mRNA is actin-dependent and requires a part of its own protein, namely the N-terminal actin-binding domain. Moreover, mRNA localization is sensitive to inhibition of translation, but only if polysomes are disrupted in the process. Taken together, these data suggest that ABP140 mRNA could localize as part of a ternary complex consisting of ribosome, mRNA, and nascent protein, which binds to actin cables.

Results

ABP140 mRNA localizes to the distal pole of the mother cell

Previous data from our group indicated that Arf1p plays a role in mRNA localization (Trautwein et al., 2004). To find additional mRNA targets of Arf1p, we used microarrays to identify transcripts that accumulate in the ER membrane-enriched 13,000 x g pellet of a temperature-sensitive *arf1* mutant if compared to wild-type. mRNAs identified in this screen were subjected to fluorescence *in situ* hybridization (FISH) to verify their subcellular localization. One of the candidate mRNAs was ABP140 mRNA.

Analyzing the FISH data, we realized that ABP140 mRNA localizes in a very distinct pattern in wild-type cells; namely, it is concentrated in one spot at the distal pole of the mother cell in about 40-50% of the cell population (Fig. 1A and B). Line plots of individual cells can be

found in the supplementary material (Suppl. Fig. 1A). Antisense probes directed against two different regions of the mRNA yielded an identical pattern. Only background signal was detected in a *Δabp140* strain, indicating that our staining was specific (Fig. 1A and B). Distal pole localization had not been described for any mRNA in yeast before and was not observed for any other of the 25 mRNAs identified in the screen that we tested.

The distal pole in *S. cerevisiae* is not very well characterized. Under favorable conditions, growth is polarized towards the bud, and many proteins and mRNAs are known to concentrate there (Lew and Reed, 1993; Long et al., 1997; Takizawa et al., 1997; Walch-Solimena et al., 1997; Shepard et al., 2003; for review, see Pruyne et al., 2004). In contrast, not a single molecule has been described to be constantly transported to the distal pole of the mother cell. However, early in daughter cell development, Bud8p is deposited at the bud tip, where it serves as a cortical landmark that is stable during several cell divisions (Harkins et al., 2001; Schenkman et al., 2002; Cullen and Sprague, 2002). Since haploid yeast cells bud in an axial pattern, meaning that each new daughter buds proximal to the birth scar (Chang and Peter, 2003), such a landmark coincides with the distal pole during the entire life of a haploid cell. Thus, we wondered whether ABP140 mRNA was recruited to a distal pole landmark or whether it would be found opposite to the current bud even if the cell repolarized. For this, we used a *Δbud5* strain that buds in a random pattern, but is not affected in Bud8p landmark deposition (Yang et al., 1997; Kang et al., 2001). As in the wild-type, ABP140 mRNA was concentrated distal to the current bud in this strain, and we observed no random distribution along the cortex of the mother cell (Suppl. Fig. 1B and C). The same was true for the diploid yeast BY4743, which buds bipolarly, i.e. polarity is reverted after each cell cycle, and for a *Δbud7/Δbud7* strain with a random budding pattern (Yang et al., 1997; Suppl. Fig. 1B and C). From this data, it was apparent that the site of ABP140 mRNA accumulation was determined by the current polarity axis of the cell.

ABP140 mRNA localization requires actin cables

The polarity of yeast cells is mostly determined by the presence of a polarized actin cytoskeleton along which protein and mRNA cargoes are transported (for review, see Pruyne et al., 2004). Thus, we wanted to know whether localization of ABP140 mRNA also depended on actin cables. We deleted the tropomyosin *TPM1* - in the resulting strain, only very few actin cables are detected (Liu and Bretscher, 1989; Suppl. Fig. 1D). In the *Δtpm1* strain, the FISH signal was diffuse and cytoplasmic, and localization to the distal pole was very rarely observed (Fig. 1C and D). To see whether short-term disruption of actin cables would have the same effect, we applied Latrunculin A (LatA), which prevents polymerization of actin (Coué et al., 1987). After only 10 min of LatA treatment, which is sufficient to abolish the actin/myosin-dependent localization of ASH1 mRNA to the bud tip, ABP140 mRNA became disperse (Takizawa et al., 1997; Fig. 1C and D). In *S. cerevisiae*, the actin cytoskeleton is also required for the proper orientation of microtubules, which have been implicated in mRNA trafficking in many organisms (Theesfeld et al., 1999; Hwang et al., 2003; Czaplinski and Singer, 2006; Cepeda-García et al., 2010). However, disruption of microtubules by treatment with benomyl did not affect the localization of ABP140 mRNA (Fig. 1C and D). Taken together, these data suggest that ABP140 mRNA could be transported to the distal pole on actin cables.

The ORF sequence is sufficient to localize ABP140 mRNA to the distal pole

In many instances, mRNAs are localized with the help of trans-acting factors that recognize sequences in the untranslated regions (UTRs) of the transcript, most often in the 3'UTR (for review, see Jambhekar and Derisi, 2007). To test whether the UTRs play a role in ABP140 mRNA localization, we replaced the endogenous sequences. When the ABP140 5'UTR was exchanged for the ADH1 promoter, the signals, which were now often elongated or crescent-

shaped, were markedly stronger, but nevertheless localized to the distal pole (Fig. 2A). Similarly, when the endogenous 3'UTR was replaced by GFP followed by the ADH1 3'UTR, ABP140 mRNA localized as in wild-type (Fig. 2A and B), and even combination of these replacements had no effect on mRNA localization, indicating that the ORF sequence was sufficient to localize the transcript (Fig. 2A and B).

ABP140 mRNA colocalizes with actin cables

The protein product of ABP140 mRNA localizes to actin cables and has been used as marker to study actin cable dynamics in yeast (Yang and Pon, 2002; Huckaba et al., 2004). As the mRNA of the GFP-tagged construct displayed wild-type localization to the distal pole, we could visualize Abp140p-labelled actin cables and ABP140 mRNA simultaneously using combined FISH/immunofluorescence (FISH/IF). Most ABP140 mRNA accumulations colocalized with actin cables (72%, n= 356), often at sites where several cables converged, again suggesting that ABP140 mRNA is transported on the actin cytoskeleton (Fig. 2C).

In *S. cerevisiae*, actin cables are polarized towards the bud, such that myosin-driven transport is predominantly directed away from the distal pole (Yang and Pon, 2002). This made it improbable that ABP140 mRNA was transported by a myosin motor. Indeed, when we deleted the unconventional myosin *MYO4*, which mediates mRNA transport to the bud tip, ABP140 mRNA localized as in wild-type (Long et al., 1997; Takizawa et al., 1997; Suppl. Fig. 2A and B). Actin cables, however, are not stationary, and insertion of actin monomers in the bud neck region results in a constant retrograde flow (Yang and Pon, 2002). Mitochondria that are retained in the mother cell during cell division have been shown to undergo actin-dependent retrograde movement at the speed of the flow, indicating that they are transported towards the distal pole by stable linkage to actin cables (Boldogh et al., 2005).

Localization of Abp140p determines ABP140 mRNA localization

If ABP140 mRNA was transported by actin retrograde flow, the machinery would - in the simplest case – require only one protein with two distinct features: An RNA-binding domain, which would be able to recruit ABP140 mRNA, and an actin-binding domain (ABD), which would stably link the mRNA to actin cables. Retrograde flow would then transport the mRNA towards the distal pole, where the mRNA would be deposited at sites where the cables disassembled.

Most actin-binding proteins in yeast are predominantly found in actin patches, structures involved in endocytosis that are concentrated in the bud region (Kübler and Riezman, 1993; Doyle and Botstein, 1996; Ayscough et al., 1997; Kaksonen et al., 2003; Huckaba et al., 2004). One protein that could meet our requirements was Abp140p itself: With an ABD located in the first 17 amino acids, it almost exclusively binds to actin cables, and brighter spots of Abp140p-GFP on cables have been used as fiduciary marks to determine the speed of actin retrograde flow (Yang and Pon, 2002; Huckaba et al., 2004; Riedl et al., 2008). In addition, Abp140p carries a putative RNA-binding domain, which we mapped to amino acids 205 to 249 using the optimal prediction mode of RNAbindR, a software for prediction of RNA-binding residues in proteins (Terribilini et al., 2007). First, we tested whether actin-binding of Abp140p was required for correct localization of ABP140 mRNA. An N-terminal truncation where the ABD was replaced by GFP localized to the cytoplasm (ΔN17-GFP-Abp140; Fig. 3A). When we assessed the mRNA localization, the staining was also cytoplasmic, indicating that actin binding of Abp140p was required for ABP140 mRNA localization to the distal pole (Fig. 3A).

Next, we asked whether we could force ABP140 mRNA into an ectopic localization if we redirected the protein to a different organelle. Therefore, we replaced the ABD of Abp140p by the C-terminus of *Listeria monocytogenes* ActA, which binds the outer mitochondrial leaflet in mammalian cells (Pistor et al., 1994). This peptide has been used previously to sequester proteins to mitochondria *in vivo* (Zhu et al., 1996; Bear et al., 2000). Interestingly,

the ActA peptide targeted Abp140p to the ER in our strain background (ActA-ABP140-GFP; Fig. 3A). ER localization of ActA-Abp140p was confirmed by coexpression of a plasmid-borne ER marker (Sec63p-RFP, Suppl. Fig. 3A). Importantly, the mRNA of this construct behaved similarly to the protein: It localized to the cell periphery and encircled the nucleus, a structure typical for yeast ER (Fig. 3A and Suppl. Fig. 3B). Colocalization of this construct's mRNA with the ER was verified by confocal microscopy using FISH/IF where we stained for the ER-marker HDEL-GFP (71% of all mRNA foci, n = 315; Suppl. Fig. 3C). From this data, it was apparent that the localization of Abp140p determined the localization of ABP140 mRNA.

To provide corroborating evidence that Abp140p expression is required to localize its mRNA, we generated a construct in which we replaced the endogenous 5'UTR of ABP140 by the ADH1 promoter followed by a GFP including a stop codon; the resulting transcript carries the full ORF, but only GFP is expressed (GFP-TAA-ABP140). The mRNA of this construct did not localize to the distal pole, but showed a punctate staining throughout the cell (Fig. 3B). Because of the artificially extended 3'UTR, there was a possibility that this construct would be a substrate for nonsense-mediated decay, which affects transcripts that carry premature stop codons (Leeds et al., 1991). However, by immunoblot, we detected expression of GFP, and quantitative RT-PCR with primers specific for ABP140 revealed that the mRNA was present in amounts comparable to the wild-type transcript when placed under the same promoter (Fig. 3C and D). Taken together, this indicated that expression of Abp140p was required to localize its mRNA to the distal pole and strengthened our notion that Abp140p directly mediates the localization of ABP140 mRNA.

The first 67 amino acids of Abp140p are sufficient to localize ABP140 mRNA

Next, we wanted to determine whether Abp140p satisfies the second requirement for our minimal model of ABP140 transport – the capacity to bind mRNA. We removed the putative

RNA-binding domain (*Δrna*). To our surprise, the mRNA localized as in wild-type (Suppl. Fig. 4A and B), indicating that ABP140 mRNA associates with Abp140p independently of the putative RNA-binding domain.

In order to identify the part of Abp140p involved in localizing its mRNA, we generated a series of C-terminal truncations. All truncations were expressed (Fig. 4A), and the protein product localized to actin cables for each of the constructs (Suppl. Fig. 4C). When we probed for the mRNAs using a probe complementary to GFP, distal pole localization was detected for all truncation constructs except for the shortest, (1-17)-GFP, demonstrating that even though the ABD was necessary, it was not sufficient to localize the mRNA (Fig. 4B and C). However, in addition to the ABD, only a very short fragment comprising amino acids 18 - 67 was required for mRNA localization.

mRNA localization is determined by the length of the translatable sequence that follows the N-terminal ABD

To verify whether amino acids 18-67 were specifically required to localize ABP140 mRNA to the distal pole, we generated a deletion mutant in which this sequence was replaced by GFP. As a control, in a second construct, GFP was inserted between amino acids 17 and 18. As expected, because the N-terminal ABD remained intact, the resulting proteins localized to actin cables (Suppl. Fig. 4D). Interestingly, the mRNA of both constructs localized as in wild-type (Fig. 5A). Thus, although amino acids 18-67 were sufficient to induce distal pole localization when added to (1-17)-GFP – which by itself does not localize the mRNA – , this sequence was not required for localization of the full-length mRNA. One possible explanation for this result is that the length of the construct is critical, regardless of the sequence. When we appended the ABD, which was not sufficient to localize the mRNA if fused to GFP alone, to four copies of GFP, this expanded construct now localized to the distal pole, although the fragment of Abp140p it contained was identical ((1-17)-4GFP; Fig. 5B and C). Conversely,

when we inserted a stop codon between amino acid 67 of Abp140p and the GFP sequence of (1-67)-GFP, mRNA localization to the distal pole was lost ((1-67)TAA-GFP; Fig. 5B and C). Thus, proper localization of ABP140 mRNA seemed to be dependent on the total length of the protein that followed the ABD, rather than on any specific sequence that the protein or the mRNA contained.

mRNA localization requires active translation

The observation that mRNA localization depends on the length of the construct made us think that transport of ABP140 mRNA could happen cotranslationally. The N-terminal ABD is the first part of the protein to exit the ribosome during translation – thus, transport could be mediated by the N-terminal domain, which is already exposed to the cytoplasm while nascent protein and mRNA are still stably associated with the translating ribosome. This way, the translating ribosome would provide the missing link between protein and mRNA, but would do so independently of the sequence that followed the localization domain. If this hypothesis was correct, we would expect that inhibition of translation would disrupt transport of ABP140 mRNA to the distal pole. Indeed, when we used the conditional allele *prt1-1*, a mutant deficient in translation initiation (Hartwell and McLaughlin, 1969), ABP140 mRNA became dispersed (Fig. 6A). Loss of translating polysomes was confirmed by polysome profile analysis (Fig. 6B). Localization of ABP140 mRNA was similarly disrupted when we treated wild-type cells with protein translation inhibitor Verrucarin A (VA), but not when we used cycloheximide (CHX), a translation inhibitor that stabilizes polyribosomes (Fig. 6C, D and G). To exclude that we depleted Abp140p during VA treatment, we detected the GFP-tagged protein by immunoblot. No decrease in Abp140p levels was observed (Fig. 6F), indicating that depletion of the protein was not responsible for the mislocalization of the mRNA.

The 3'UTR of ASH1 mRNA, a transcript that localizes to the bud tip with help of a specialized actin/myosin system, has been shown to be sufficient to induce bud tip

localization if added to another mRNA (Long et al., 1997; Takizawa et al., 1997). When we replaced the endogenous 3' UTR of ABP140 with ASH1 3'UTR, it was unable to induce bud tip localization, and the transcript localized to the distal pole almost as efficiently as wild-type (Fig. 6E and G). However, when we treated the cells with the translational inhibitor VA, dominance of distal pole localization was lost, and the mRNA was now found at the bud tip in 30-40 % of the population (Fig. 6E and G). In contrast, CHX treatment did not confer bud tip localization (Fig. 6E and G). Taken together, these experiments suggest that association of ABP140 mRNA with ribosomes is necessary for distal pole localization, supporting the cotranslational transport.

+1 ribosomal frameshift is not required for ABP140 mRNA localization

ABP140 mRNA carries a +1 ribosomal frameshift site at amino acid 277. The frameshifting mechanism involves a translational pause at a codon that is recognized very slowly. Recognition of the first codon in the +1 frame by a highly abundant tRNA then leads to a shift in the reading frame (Farabaugh et al., 2006). Thus, we hypothesized that this translational pause might increase the efficiency of cotranslational transport of ABP140-mRNA. A frameshift-corrected allele of *ABP140* (similar to Morris and Lundblad, 1997), however, localized as in wild-type (*abp140-RFS**; Suppl. Fig. 5A and B), demonstrating that the frameshift site did not significantly enhance mRNA localization. If frameshifting on Abp140 fails, translation is terminated at a stop codon immediately downstream of the frameshift site, which results in a C-terminally truncated protein that is easily distinguished from full-length Abp140p by immunoblot when an internal GFP-tag is inserted (Suppl. Fig. 5C and D). Interestingly, frameshifting efficiency of Ty1 retrotransposon, which carries an identical frameshift site, is largely dependent on the growth condition and increases after diauxic shift, due to variations in tRNA availability (Stahl et al., 2004). However, the ratio between non-frameshifted, truncated Abp140p and the frameshifted full-length protein did not increase

when cells entered stationary phase (Suppl. Fig. 5E). In addition, expression of the frameshift mutant *abp140-RFS**, which produces only full-length Abp140p, had no deleterious effect when cells were grown on glycerol, indicating that differential frameshifting on Abp140p is not part of a regulatory mechanism during diauxic shift (unpublished observation). Depending on the demand, the local availability of tRNAs can vary (Zhang et al., 2010). Thus, we hypothesized that the high local concentration of ABP140 mRNA at the distal pole may lead to a depletion of factors at the site, which in turn might impact on frameshifting efficiencies. To test this, we deleted *TPM1* in a strain expressing internally GFP-tagged Abp140p. Because actin cables are absent in this strain, Abp140p relocalizes to actin patches, and ABP140 mRNA is uniformly distributed throughout the cell (Suppl. Fig. 5F; see Fig. 1C). However, we could detect no significant difference to the wild-type (Suppl. Fig. 5E), indicating that concentration at the distal pole had no influence on frameshifting efficiencies.

ABP140 mRNA localization is dynamic and follows movements of the actin cytoskeleton

To further support our model, we wanted to follow ABP140 mRNA movement on actin cables. For live tracking of mRNAs, different systems have been developed that rely on stemloop structures that can be integrated into the mRNA and are detected with the help of fluorescently tagged stemloop-binding proteins (Bertrand et al., 1998; Brodsky and Silver, 2000). We integrated either MS2 or U1A stemloops into the 3'UTR of ABP140 mRNA and followed the fluoresecence using plasmid-borne MS2-GFP or U1A-GFP, respectively (Fig. 7A). Since ABP140 mRNA localization was more prominent when cells were grown in rich medium, and the U1A-GFP plasmid was only poorly retained under these conditions, we used the MS2 system for timelapse imaging. Most frequently, MS2-GFP was observed in elongated structures that hovered around the distal pole (Suppl. Movies 1 and 2), but rapid linear movements of particles or filaments from the distal pole to the bud neck region and in reverse direction were similarly observed (Fig. 7B, C and D, Suppl. Movies 3, 4 and 5).

During long-range movements, particles crossed the mother cell in 3-6 frames, which approximately matches the published speed of actin cable elongation of ~0.3 μm/s (Yang and Pon, 2002). In 169 cells that were filmed for 270 s on average, we observed 25 cases of fast long-range movement directed towards the bud neck (e.g. Suppl. Movie 6), 19 cases of fast long-range movements directed towards the distal pole (e.g. Suppl. Movie 3, Fig. 7B and C), 22 cases of looping (where the signal quickly traversed the cell but immediately returned to its place of origin on another route, e.g. Suppl. Movies 4 and 5, Suppl. Fig. 6), and 9 cases of fast lateral cable movements (e.g. Suppl. Movie 7). When ABP140-MS2/MS2-GFP was followed in the presence of an actin cable marker, plasmid-borne Abp140(1-17)-2xmCherry, the GFP signal was observed to colocalize with brighter patches on actin cables (Fig. 7E, Suppl. Movies 6 and 7). Collectively, our data strongly support a model of cotranslational transport of ABP140 mRNA to the distal pole via actin retrograde flow.

Discussion

As a somewhat unexpected finding, we identified ABP140 mRNA as the first distal pole-localized transcript in *S. cerevisiae* in a screen for mRNAs that change localization in an *ARF1* mutant. The effect of the *arf1-11* mutation on ABP140 localization is likely indirect, because this mutant shows a decrease in general translation at the restrictive temperature (Kilchert et al., 2010). However, ARF proteins were shown to play a role in the organization of the actin cytoskeleton (Myers and Casanova, 2008).

We suggest that ABP140 mRNA is transported to the distal pole cotranslationally by actin retrograde flow, as part of the ternary complex of mRNA, translating ribosome, and nascent polypeptide (Fig. 8). The ABD of Abp140p is sufficient to localize the mRNA if appended to any long translatable sequence that keeps the translating complex stable while the ABD is exposed. Longer mRNAs also accommodate more ribosomes. The sum of nascent peptides can bind actin with avidity, enhancing the recruitment to cables.

Alternative models are conceivable: The sequence encoding the ABD could contain an RNA recognition motif recognized by another factor, which would link the mRNA to actin cables, leading to the impression that actin-binding of Abp140p was required for localization of its mRNA. This factor could be rapidly depleted after translational shut-down, thereby abolishing distal pole localization under these conditions. However, if translation was shut down with CHX, which stabilizes the ternary complex, distal pole localization was maintained (Fig. 6). Moreover, we have generated at least three constructs which contain the ABD, but do not localize to the distal pole. In addition, the data on ActA-Abp140 suggests that localization of Abp140p and its mRNA are correlated (Fig. 3).

We consider the presence of a third factor unlikely. First, the ABD is sufficient to localize the mRNA if a long translated sequence follows. Second, we were unable to rescue localization of non-localizing constructs *in trans*, by coexpressing wild-type Abp140p ((1-17)-mCherry or (1-67)TAA-GFP; unpublished observation). Third, on the RNA level, the molecular differences between the constructs are much smaller than on the protein level.

Our findings complement other cotranslational mechanisms that have been reported previously (Walter and Blobel, 1981; Ahmed and Fisher, 2009; Yanagitani et al., 2009; Garcia et al., 2010; Liao et al., 2011). During targeting of signal recognition particle (SRP)-dependent mRNAs to the ER, SRP recognizes the nascent peptide and halts translation until bound by the SRP receptor (Walter and Blobel, 1981). Mammalian XBP1, an mRNA that is spliced in response to ER stress, is tethered to the ER by hydrophobic regions contained solely in the unspliced protein product. In this case, a conserved peptide in the C-terminus stably interacts with the protein-conducting channel of the ribosome, and this induced translational pause is thought to maintain the ternary complex stable (Yanagitani et al., 2009; Yanagitani et al., 2011). For ABP140, we found no evidence that a specific region of the protein would be required to slow down protein synthesis in order to allow cotranslational transport. As far as we know, mRNA localization may be an intrinsic property that would be

shared by any protein with a domain structure similar to Abp140p, with a protein interaction domain close to the N-terminus, and might occur much more frequently than is currently appreciated. Lécuyer et al. (2007) found most transcripts in *Drosophila* oocytes and early embryos to be subcellularly enriched, and the localization of the mRNAs matched that of their protein products in most of the cases. For many of these, mRNA localization might not require a dedicated machinery, but may simply happen as a by-product of translation in the cytoplasm, where nascent proteins are already exposed to interactors. mRNAs may thus have a tendency to accumulate at sites where their protein product encounters binding partners. On a very speculative note, if such translation *in situ* would enhance the efficiency of protein sorting, this could even favor the evolution of N-terminal protein interaction domains over alternative domain arrangements.

We found the speed of ABP140 mRNA movement to be consistent with the reported speed of actin flow (Yang and Pon, 2002; Fig. 7). In contrast to Yang and Pon, we also observed movement of cables towards the bud neck, which could be due to the required overexpression of Abp140p, which might alter actin dynamics (Gao and Bretscher, 2008). In addition, recent data indicate that not all actin filaments are strictly polarized (Yu et al., 2011). In accordance with this, MS2-GFP foci frequently looped back to the distal pole on a different route shortly after they had reached the bud neck. Thus, the steady state localization of ABP140 mRNA represented in the FISH may reflect the degree of predominance of filaments polarized towards the bud over filaments with reverted polarity.

To date, the function of Abp140p remains largely elusive. Its best characterized features are the ABD with its weak actin-bundling activity (Asakura et al., 1998; Yang and Pon, 2002; Riedl et al., 2008) and the highly conserved C-terminal methyltransferase domain, which has recently been shown to mediate methylation of tRNAs (Farabaugh et al., 2006; D'Silva et al., 2011; Noma et al., 2011). These seemingly unrelated functions are separated by the ribosomal frameshift site (Farabaugh et al., 2006). The ABD is conserved only among close relatives of

budding yeast, but not found in other organisms (Riedl et al., 2008). *ABP140* shows physical and genetic interactions with regulators of Rho GTPase activity, the septin ring, and factors involved in actin polymerization and stabilization (Gao and Bretscher, 2008; Costanzo et al., 2010; Michelot et al., 2010), supporting a possible role of Abp140p in actin dynamics.

While ABP140 mRNA is predominantly found close to the distal pole, Abp140p appears to be associated with cables throughout the cell. However, when we fused an aggregation-prone red fluorescent protein C-terminally to Abp140p, the protein accumulated at the distal ends of actin cables (Suppl. Fig. 7A and B), indicating that the mRNA at the distal pole might be the primary source of the protein. It has been reported to be beneficial for the assembly of some large protein complexes if their components are generated close by (Chang et al., 2006; Halbach et al., 2009). In the case of Abp140p, the situation would be the opposite, as actin cables are thought to polymerize at the bud neck. However, the bud region is packed with other actin structures, including actin patches. There is a possibility that cotranslational enrichment at the distal pole could favor association of Abp140p with actin cables over integration into actin patches. For (1-17)-Abp140p-GFP, we observe patch staining in addition to actin cable staining (Suppl. Fig. 4C), which we never detected for any of the mRNA localizing constructs. This is not simply due to the small size of the protein, because full-length Abp140p also becomes integrated into patches in the *Δtpm1* strain, where cables are largely absent, and in which the mRNA, again, does not localize (Fig. 1C and Suppl. Fig. 5E). In agreement with this, Michelot et al. (2010) have found Abp140p to interact with the actin patch protein Las17p. If this model was true, it could explain why C-terminal truncation does not gradually decrease localization efficiency, but becomes catastrophic at a certain point: Enhanced integration of the nascent protein into patches would further decrease distal pole localization of the mRNA, resulting in a negative feedback loop. Since Abp140p has actin-bundling activity, excessive integration of the full-length protein into patches could potentially disrupt their function. We are not able to test this hypothesis, however, since other

RNA localization signals, e.g. the ASH1-3'UTR, were not strong enough to mislocalize the transcript. Thus, we cannot express full-length Abp140p at a different location without disrupting the actin cytoskeleton.

Materials and Methods

Yeast methods

Standard genetic techniques were employed throughout (Sherman, 1991). All genetic manipulations were performed chromosomally. Tagging and deletions were carried out as described (Knop et al., 1999; Gueldener et al., 2002; Janke et al., 2004; Gauss et al., 2005). The *RFS** and the *Δrna* mutant were generated with the delitto perfetto method (Storici et al., 2001). To N-terminally insert the ActA peptide, oligonucleotides CK496/496 containing the ActA N-terminal were inserted into pYM-N7, which was used as a template for the integration cassette. ASH1-3'UTR was subcloned from YEP lac195 Lz-MS2-Ash1 (Bertrand et al., 1998) into pYM27 to allow chromosomal tagging. Similarly, MS2 and U1A stemloops were integrated into pYM51 to allow cassette amplification and chromosomal integration. NLS-MS2-GFP was subcloned from pG14-MS2-GFP (Bertrand et al., 1998) into p415 ADH (Mumberg et al., 1995) to reduce the expression level. All yeast strains are given in Table S1, and primers and plasmids (including a detailed description of their generation) used for strain construction are given in Tables S2 and S3, respectively.

None of the strains used in this study had a marked growth phenotype on YPD, nor did they appear very sick/misshaped under the microscope. Importantly, this was also true for all strains in which ABP140 mRNA was mislocalized (Suppl. Fig. 7C). Since we knew that actin-binding of Abp140p was required for mRNA localization, we routinely tested whether our constructs localized to actin cables using GFP fusions (Suppl. Fig. 8A unless shown elswhere); in doing this, we also confirmed that actin cable integrity was not affected in these strains. In strains where we could not insert a GFP tag or where the construct was designed to

not bind to cables (DN17-Abp140, GFP-TAA-Abp140, ActA-Abp140, (1-67)TAA-GFP), we used rhodamine phalloidin staining to verify that the actin cytoskeleton was intact (Suppl. Fig. 8B). There was only one strain in which the morphology of the actin cytoskeleton was clearly altered: In (1-17)-4GFP, about 10-20% of all cells contained a massive bundle of actin cables that was oriented perpendicular to the mother-daughter axis (Suppl. Fig. 8A). In the *Δtpm1* strain, with no cables present, Abp140-GFP relocalized to the sites of polarized growth, presumably to actin patches (Suppl. Fig. 5F). (1-17)-GFP showed some patch staining in addition to the usual localization to actin cables (Suppl. Fig. 4C).

Fluorescent in situ hybridization (FISH)

In situ mRNA hybridization with digoxigenin-labeled antisense probe was performed as described previously (Takizawa et al., 1997). Primers used for probe generation are given in Table S2. Fluorescence was monitored with an Axiocam mounted on an Axioplan 2 fluorescence microscope (Carl Zeiss, Oberkochen, Germany) using an eqFP611 filter (AHF analysentechnik, Tübingen, Germany) and Axiovision software. For quantitation, only budded cells were counted, and only those cells where mother/daughter pairs could be unambiguously assigned in the DIC channel were considered. All cells where the brightest signal was close to the cortex in an area spanning 60° to both sides of the central axis, either dot- or crescent-shaped, were considered positive. For every condition, a minimum of one hundred cells from at least two independent experiments was counted. 95.4% confidence intervals were determined assuming random sampling and using the normal approximation for a binomial distribution. Statistical significance was tested using a one-tailed two proportion z-test.

Combined FISH/immunofluorescence

An adapted protocol was used for combined FISH/immunofluorescence. In short, 2.5 OD of yeast cells grown to logarithmic phase were fixed with 3.6 % formaldehyde for 1h at RT, washed twice in PBS, and resuspended in 100 mM KP_i (pH 7.0), 1.2 M sorbitol. After 5 min pretreatment with 30 mM 2-mercaptoethanol, cells were spheroplasted with zymolyase T-100 (Seikagaku Biobusiness). Cells were washed repeatedly in 100 mM KP_i (pH 7.0), 1.2 M sorbitol, and left to settle on poly-lysine-treated slides. The slides were fixed by immersion in ice-cold methanol for 6 min, then in ice-cold acetone for 30 s, and air-dried. Prehybridization and hybridization were carried out according to the standard FISH protocol. After hybridization, slides were washed 2 x 10 min with 0.5 x SSC pre-warmed to 42°C. Wells were washed with PBT (PBS, 0.1% Tween-20; 1 x 5 min) and blocked with PBTB (PBS, 0.1% Tween-20, 1% non-fat milk) for 10 min. Incubation with anti-DIG-POD (Roche, 1:750 in PBTB) and anti-GFP (Torrey Pines, 1:200) was carried out for 1 h at 37°C in a humid chamber. Wells were washed repeatedly with PBTB (6 x 5 min) and subsequently incubated with preabsorbed chicken anti-rabbit-IgG-Alexa488 (Invitrogen, 1:200 in PBS) for 1 h at 37°C in a humid chamber. After repeated washing (3 x 5 min PBTB, 1 x 5 min PBT, 1 x 5 min PBS), 10 µl tyramide solution (PerkinElmer, 1:100 in Amplification Solution) was added to each well and incubated for 1 h at 37°C in a humid chamber. Slides were washed with PBS (6 x 5 min), and mounted with Citifluor AF1 (supplemented with 1 µg/ml DAPI to stain the nuclei). Pictures were taken on a Leica SP5 confocal microscope. Image processing was performed with ImageJ (NIH, open source).

Live-cell imaging

Yeast cells were grown in YPD to early log phase. The cells were taken up in HC-complete medium containing 2% glucose and immobilized on ConA-coated slides. Fluorescence was monitored with an Axiocam mounted on an Axioplan 2 fluorescence microscope (Carl Zeiss, Oberkochen, Germany) using GFP and eqFP611 filters (AHF analysentechnik, Tübingen,

Germany) and Axiovision software. For time-lapse imaging, pictures of all three channels were acquired every 10s, with exposure times of 250 ms (RFP), 500 ms (GFP), or set to automatic acquire mode (DIC). Movies display the images at 50 frames per second and were generated with ImageJ.

Denaturing Yeast Extracts and Western Blot Quantitation

15 ml of yeast culture were grown to early log phase (OD_{600} 0.5–0.7). The cells were harvested and lysed with glass beads in 150 µl of lysis buffer (20 mM Tris/HCl pH8, 5mM EDTA, 1mM DTT, 1% SDS). The lysates were incubated at 65°C for 5 min and cell debris removed by centrifugation. Per sample, 30 µg of the lysate were analyzed by SDS-PAGE and immunoblotting using polyclonal rabbit anti-GFP antibodies (1:1000, Torrey Pines). For quantitation of frameshifting efficiences, lysates were generated with Lämmli containing 8M Urea to allow efficient disruption of stationary cells and 2 µl of total lysate were loaded per lane. Band intensities were quantified using the ImageQuant LAS 4000 system (GE Healthcare).

quantitative real-time PCR

For qPCR, total RNA was isolated from yeast essentially as described (Schmitt et al., 1990). RNA clean-up and qPCR were carried out at the Life Sciences Training Facility (LSTF) of the University of Basel. In short, 5 µg of RNA were treated with Turbo DNase (*TURBO* DNA-free™ Kit, Ambion), cleaned up on Zymo-Spin™ columns (Zymo Research), and reverse transcribed using random nonamers and the Eurogentec Core Kit (RT-RTCK-03). The resulting cDNA was used as a template for the qPCR reaction and incorporation of SyBR green monitored on a Corbett Rotor-Gene Q. *PGK1* was used as reference gene. The primers used for the qPCR reaction are given in Table S2.

Polysome profiles

Polysome preparations were performed as described previously (de la Cruz et al., 1997) on 4–47% sucrose gradients prepared with a Gradient Master (Nycomed Pharma, Westbury, NY). Gradient analysis was performed using a gradient fractionator (Labconco, Kansas City, MO) and the Äcta FPLC system (GE Healthcare) and continuously monitored at A_{254}

Acknowledgments

We are very grateful to P. Lappalainen, C.-A. Schönenberger, U. Silvan, R. Wedlich-Söldner and members of the Spang lab for discussions. We also appreciate the contribution of P. Demougin, who helped with the qPCR experiment, and of J. Weidner, who optimized the protocol for the combined FISH/immunofluorescence. The Sec63p-RFP plasmid was kindly provided by S. Michaelis and pYM-4GFP-Kan was a gift of C. Taxis. We thank B. Glick, P. Chartrand, J. Hegemann, M. Knop, A. Nakano, R. Parker, M.A. Resnick, S. Rospert, E. Schiebel and P. Silver for strains and reagents. This work was supported by the Boehringer Ingelheim Fonds (C.K.), the Human Frontier Science Program, the Swiss National Fund, and the University of Basel.

Author contributions

CK and AS designed the study and interpreted the results. CK performed the experiments and analyzed the data. CK and AS wrote and edited the manuscript.

Supplementary information is available at The EMBO Journal Online.

References

Ahmed AU, Fisher PR (2009) Import of nuclear-encoded mitochondrial proteins: a cotranslational perspective. *Int Rev Cell Mol Biol.* **273**:49-68.

Aronov S, Gelin-Licht R, Zipor G, Haim L, Safran E, Gerst JE (2007) mRNAs encoding polarity and exocytosis factors are cotransported with the cortical endoplasmic reticulum to the incipient bud in Saccharomyces cerevisiae. *Mol Cell Biol.* **27**:3441-55.

Aronov S, Gerst JE (2004) Involvement of the late secretory pathway in actin regulation and mRNA transport in yeast. *J Biol Chem.* **279**:36962-71.

Asakura T, Sasaki T, Nagano F, Satoh A, Obaishi H, Nishioka H, Imamura H, Hotta K, Tanaka K, Nakanishi H, Takai Y (1998) Isolation and characterization of a novel actin filament-binding protein from Saccharomyces cerevisiae. *Oncogene* **16**:121-30.

Ayscough KR, Stryker J, Pokala N, Sanders M, Crews P, Drubin DG (1997) High rates of actin filament turnover in budding yeast and roles for actin in establishment and maintenance of cell polarity revealed using the actin inhibitor latrunculin-A. *J Cell Biol.* **137**:399-416.

Bear JE, Loureiro JJ, Libova I, Fässler R, Wehland J, Gertler FB (2000) Negative regulation of fibroblast motility by Ena/VASP proteins. *Cell* **101**:717-28.

Bertrand E, Chartrand P, Schaefer M, Shenoy SM, Singer RH, Long RM (1998) Localization of ASH1 mRNA particles in living yeast. *Mol Cell.* **2**:437-45.

Bi J, Tsai NP, Lu HY, Loh HH, Wei LN (2007) Copb1-facilitated axonal transport and translation of kappa opioid-receptor mRNA. *Proc Natl Acad Sci U S A.* **104**:13810-5.

Blower MD, Feric E, Weis K, Heald R (2007) Genome-wide analysis demonstrates conserved localization of messenger RNAs to mitotic microtubules. *J Cell Biol.* **179**:1365-73.

Boldogh IR, Fehrenbacher KL, Yang HC, Pon LA (2005) Mitochondrial movement and inheritance in budding yeast. *Gene* **354**:28-36.

Brodsky AS, Silver PA (2000) Pre-mRNA processing factors are required for nuclear export. *RNA* **6**:1737-49.

Cepeda-García C, Delgehyr N, Ortiz MA, ten Hoopen R, Zhiteneva A, Segal M (2010) Actin-mediated delivery of astral microtubules instructs Kar9p asymmetric loading to the bud-ward spindle pole. *Mol Biol Cell.* **21**:2685-95.

Chang F, Peter M (2003) Yeasts make their mark. *Nat Cell Biol.* **5**:294-9.

Chang L, Shav-Tal Y, Trcek T, Singer RH, Goldman RD (2006) Assembling an intermediate filament network by dynamic cotranslation. *J Cell Biol.* **172**:747-58.

Costanzo M, Baryshnikova A, Bellay J, Kim Y, et al., Boone C (2010) The genetic landscape of a cell. *Science* **327**:425-31.

Coué M, Brenner SL, Spector I, Korn ED (1987) Inhibition of actin polymerization by latrunculin A. *FEBS Lett.* **213**:316-8.

Cullen PJ, Sprague GF (2002) The roles of bud-site-selection proteins during haploid invasive growth in yeast. *Mol Biol Cell.* **13**:2990-3004.

Czaplinski K, Singer RH (2006) Pathways for mRNA localization in the cytoplasm. *Trends Biochem Sci.* **31**:687-93.

de la Cruz J, Iost I, Kressler D, Linder P (1997) The p20 and Ded1 proteins have antagonistic roles in eIF4E-dependent translation in Saccharomyces cerevisiae. *Proc Natl Acad Sci U S A.* **94**:5201-6.

Diehn M, Eisen MB, Botstein D, Brown PO (2000) Large-scale identification of secreted and membrane-associated gene products using DNA microarrays. *Nat Genet.* **25**:58-62.

Doyle T, Botstein D (1996) Movement of yeast cortical actin cytoskeleton visualized in vivo. *Proc Natl Acad Sci U S A.* **93**:3886-91.

D'Silva S, Haider SJ, Phizicky EM (2011) A domain of the actin binding protein Abp140 is the yeast methyltransferase responsible for 3-methylcytidine modification in the tRNA anti-codon loop. *RNA* Epub ahead of print.

D'Souza-Schorey C, Chavrier P (2006) ARF proteins: roles in membrane traffic and beyond. *Nat Rev Mol Cell Biol.* **7**:347-58.

Farabaugh PJ, Kramer E, Vallabhaneni H, Raman A (2006) Evolution of +1 programmed frameshifting signals and frameshift-regulating tRNAs in the order Saccharomycetales. *J Mol Evol.* **63**:545-61.

Frank J (2003) Toward an understanding of the structural basis of translation. *Genome Biol.* **4**:237.

Gao L, Bretscher A (2008) Analysis of unregulated formin activity reveals how yeast can balance F-actin assembly between different microfilament-based organizations. *Mol Biol Cell.* **19**:1474-84.

Garcia M, Delaveau T, Goussard S, Jacq C (2010) Mitochondrial presequence and open reading frame mediate asymmetric localization of messenger RNA. *EMBO Rep.* **11**:285-91.

Gauss R, Trautwein M, Sommer T, Spang A (2005) New modules for the repeated internal and N-terminal epitope tagging of genes in Saccharomyces cerevisiae. *Yeast* **22**:1-12.

Gueldener U, Heinisch J, Koehler GJ, Voss D, Hegemann JH (2002) A second set of loxP marker cassettes for Cre-mediated multiple gene knockouts in budding yeast. *Nucleic Acids Res.* **30**:e23.

Halbach A, Zhang H, Wengi A, Jablonska Z, Gruber IM, Halbeisen RE, Dehé PM, Kemmeren P, Holstege F, Géli V, Gerber AP, Dichtl B (2009) Cotranslational assembly of the yeast SET1C histone methyltransferase complex. *EMBO J.* **28**:2959-70.

Harkins HA, Pagé N, Schenkman LR, De Virgilio C, Shaw S, Bussey H, Pringle JR (2001) Bud8p and Bud9p, proteins that may mark the sites for bipolar budding in yeast. *Mol Biol Cell.* **12**:2497-518.

Hartwell LH, McLaughlin CS (1969) A mutant of yeast apparently defective in the initiation of protein synthesis. *Proc Natl Acad Sci U S A.* **62**:468-74.

Holt CE, Bullock SL (2009) Subcellular mRNA localization in animal cells and why it matters. *Science* **326**:1212-6.

Huckaba TM, Gay AC, Pantalena LF, Yang HC, Pon LA (2004) Live cell imaging of the assembly, disassembly, and actin cable-dependent movement of endosomes and actin patches in the budding yeast, Saccharomyces cerevisiae. *J Cell Biol.* **167**:519-30.

Huckaba TM, Lipkin T, Pon LA (2006) Roles of type II myosin and a tropomyosin isoform in retrograde actin flow in budding yeast. *J Cell Biol.* **175**:957-69.

Hwang E, Kusch J, Barral Y, Huffaker TC (2003) Spindle orientation in Saccharomyces cerevisiae depends on the transport of microtubule ends along polarized actin cables. *J Cell Biol.* **161**:483-8.

Jambhekar A, Derisi JL (2007) Cis-acting determinants of asymmetric, cytoplasmic RNA transport. *RNA* **13**:625-42.

Janke C, Magiera MM, Rathfelder N, Taxis C, Reber S, Maekawa H, Moreno-Borchart A, Doenges G, Schwob E, Schiebel E, Knop M (2004) 'A versatile toolbox for PCR-based tagging of yeast genes: new fluorescent proteins, more markers and promoter substitution cassettes.', *Yeast*, pp. **21**:947-62.

Kaksonen M, Sun Y, Drubin DG (2003) A pathway for association of receptors, adaptors, and actin during endocytic internalization. *Cell* **115**:475-87.

Kang PJ, Sanson A, Lee B, Park HO (2001) A GDP/GTP exchange factor involved in linking a spatial landmark to cell polarity. *Science* **292**:1376-8.

Kilchert C, Weidner J, Prescianotto-Baschong C, Spang A (2010) Defects in the secretory pathway and high Ca2+ induce multiple P-bodies. *Mol Biol Cell.* **21**:2624-38.

Knop M, Siegers K, Pereira G, Zachariae W, Winsor B, Nasmyth K, Schiebel E (1999) Epitope tagging of yeast genes using a PCR-based strategy: more tags and improved practical routines. *Yeast* **15**:963-72.

Kübler E, Riezman H (1993) Actin and fimbrin are required for the internalization step of endocytosis in yeast. *EMBO J.* **12**:2855-62.

Lécuyer E, Yoshida H, Parthasarathy N, Alm C, Babak T, Cerovina T, Hughes TR, Tomancak P, Krause HM (2007) Global analysis of mRNA localization reveals a prominent role in organizing cellular architecture and function. *Cell* **131**:174-8.

Leeds P, Peltz SW, Jacobson A, Culbertson MR (1991) The product of the yeast UPF1 gene is required for rapid turnover of mRNAs containing a premature translational termination codon. *Genes Dev.* **5**:2303-14.

Lerner RS, Seiser RM, Zheng T, Lager PJ, Reedy MC, Keene JD, Nicchitta CV (2003) Partitioning and translation of mRNAs encoding soluble proteins on membrane-bound ribosomes. *RNA* **9**:1123-37.

Lew DJ, Reed SI (1993) Morphogenesis in the yeast cell cycle: regulation by Cdc28 and cyclins. *J Cell Biol.* **120**:1305-2.

Liao G, Ma X, Liu G (2011) An RNA-zipcode-independent mechanism that localizes Dia1 mRNA to the perinuclear ER through interactions between Dia1 nascent peptide and Rho-GTP. *J Cell Sci.* **124**:589-99.

Lin Y, Lu J, Zhang J, Walter W, Dang W, Wan J, Tao S, Qian J, Zhao Y, Boeke J, Berger S, Zhu H (2009) Protein acetylation microarray reveals that NuA4 controls key metabolic target regulating gluconeogenesis. *Cell* **136**:1073-84.

Liu HP, Bretscher A (1989) Disruption of the single tropomyosin gene in yeast results in the disappearance of actin cables from the cytoskeleton. *Cell* **57**:233-42.

Liu B, Larsson L, Caballero A, Hao X, Oling D, Grantham J, Nyström T (2010) The polarisome is required for segregation and retrograde transport of protein aggregates. *Cell* **140**:257-67.

Long RM, Singer RH, Meng X, Gonzalez I, Nasmyth K, Jansen RP (1997) Mating type switching in yeast controlled by asymmetric localization of ASH1 mRNA. *Science* **277**:383-7.

Marc P, Margeot A, Devaux F, Blugeon C, Corral-Debrinski M, Jacq C (2002) Genome-wide analysis of mRNAs targeted to yeast mitochondria. *EMBO Rep.* **3**:159-64.

Matlack KE, Walter P (1995) The 70 carboxyl-terminal amino acids of nascent secretory proteins are protected from proteolysis by the ribosome and the protein translocation apparatus of the endoplasmic reticulum membrane. *J Biol Chem.* **270**:6170-80.

Meignin C, Davis I (2010) Transmitting the message: intracellular mRNA localization *Curr Opin Cell Biol.* **22**:112-9.

Mili S, Moissoglu K, Macara IG (2008) Genome-wide screen reveals APC-associated RNAs enriched in cell protrusions. *Nature* **453**:115-9.

Morris DK, Lundblad V (1997) Programmed translational frameshifting in a gene required for yeast telomere replication. *Curr Biol.* **7**:969-76.

Mumberg D, Müller R, Funk M (1995) Yeast vectors for the controlled expression of heterologous proteins in different genetic backgrounds. *Gene* **156**:119-22.

Noma A, Yi S, Katoh T, Takai Y, Suzuki T, Suzuki T (2011) Actin-binding protein ABP140 is a methyltransferase for 3-methylcytidine at position 32 of tRNAs in Saccharomyces cerevisiae. *RNA* Epub ahead of print.

Pistor S, Chakraborty T, Niebuhr K, Domann E, Wehland J (1994) The ActA protein of Listeria monocytogenes acts as a nucleator inducing reorganization of the actin cytoskeleton. *EMBO J.* **13**:758-63.

Pruyne D, Legesse-Miller A, Gao L, Dong Y, Bretscher A (2004) Mechanisms of polarized growth and organelle segregation in yeast. *Annu Rev Cell Dev Biol.* **20**:559-91.

Ptacek J, Devgan G, Michaud G, Zhu H, Zhu X, Fasolo J, Guo H, Jona G, Breitkreutz A, Sopko R, McCartney R, Schmidt M, Rachidi N, Lee S, Mah A, Meng L, Stark M, Stern D, De Virgilio C, Tyers M et al. (2005) Global analysis of protein phosphorylation in yeast. *Nature* **438**:679-84.

Riedl J, Crevenna AH, Kessenbrock K, Yu JH, Neukirchen D, Bista M, Bradke F, Jenne D, Holak TA, Werb Z, Sixt M, Wedlich-Söldner R (2008) Lifeact: a versatile marker to visualize F-actin. *Nat Methods.* **5**:605-7.

Saint-Georges Y, Garcia M, Delaveau T, Jourdren L, Le Crom S, Lemoine S, Tanty V, Devaux F, Jacq C (2008) Yeast mitochondrial biogenesis: a role for the PUF RNA-binding protein Puf3p in mRNA localization. *PLoS One* **3**:e2293.

Schenkman LR, Caruso C, Pagé N, Pringle JR (2002) The role of cell cycle-regulated expression in the localization of spatial landmark proteins in yeast. *J Cell Biol.* **156**:829-41.

Schmitt ME, Brown TA, Trumpower BL (1990) A rapid and simple method for preparation of RNA from Saccharomyces cerevisiae. *Nucleic Acids Res.* **18**:3091-2.

Shepard KA, Gerber AP, Jambhekar A, Takizawa PA, Brown PO, Herschlag D, DeRisi JL, Vale RD (2003) Widespread cytoplasmic mRNA transport in yeast: identification of 22 bud-localized transcripts using DNA microarray analysis. *Proc Natl Acad Sci U S A.* **100**:11429-34.

Sherman F (1991) Getting started with yeast *Methods Enzymol* **194**:3-21.

Slobodin B, Gerst JE (2010) A novel mRNA affinity purification technique for the identification of interacting proteins and transcripts in ribonucleoprotein complexes. *RNA* **16**:2277-90.

Stahl G, Salem SN, Chen L, Zhao B, Farabaugh PJ (2004) Translational accuracy during exponential, postdiauxic, and stationary growth phases in Saccharomyces cerevisiae. *Eukaryot Cell.* **3**:331-8.

Storici F, Lewis LK, Resnick MA (2001) In vivo site-directed mutagenesis using oligonucleotides. *Nat Biotechnol.* **19**:773-6.

Takizawa PA, Sil A, Swedlow JR, Herskowitz I, Vale RD (1997) Actin-dependent localization of an RNA encoding a cell-fate determinant in yeast. *Nature* **389**:90-3.

Terribilini M, Sander JD, Lee JH, Zaback P, Jernigan RL, Honavar V, Dobbs D (2007) RNABindR: a server for analyzing and predicting RNA-binding sites in proteins. *Nucleic Acids Res.* **35**:W578-W584.

Theesfeld CL, Irazoqui JE, Bloom K, Lew DJ (1999) The role of actin in spindle orientation changes during the Saccharomyces cerevisiae cell cycle. *J Cell Biol.* **146**:1019-32.

Trautwein M, Dengjel J, Schirle M, Spang A (2004) Arf1p provides an unexpected link between COPI vesicles and mRNA in Saccharomyces cerevisiae. *Mol Biol Cell.* **15**:5021-37.

Tsvetanova NG, Klass DM, Salzman J, Brown PO (2010) Proteome-wide search reveals unexpected RNA-binding proteins in Saccharomyces cerevisiae. *PLoS One* **5**. pii: e12671.

Walch-Solimena C, Collins RN, Novick PJ (1997) Sec2p mediates nucleotide exchange on Sec4p and is involved in polarized delivery of post-Golgi vesicles. *J Cell Biol.* **137**:1495-509.

Walter P, Blobel G (1981) Translocation of proteins across the endoplasmic reticulum III. Signal recognition protein (SRP) causes signal sequence-dependent and site-specific arrest of chain elongation that is released by microsomal membranes. *J Cell Biol.* **91**:557-61.

Yanagitani K, Imagawa Y, Iwawaki T, Hosoda A, Saito M, Kimata Y, Kohno K (2009) Cotranslational targeting of XBP1 protein to the membrane promotes cytoplasmic splicing of its own mRNA. *Mol Cell.* **34**:191-200.

Yanagitani K, Kimata Y, Kadokura H, Kohno K (2011) Translational pausing ensures membrane targeting and cytoplasmic splicing of XBP1u mRNA. *Science* **331**:586-.

Yang S, Ayscough KR, Drubin DG (1997) A role for the actin cytoskeleton of Saccharomyces cerevisiae in bipolar bud-site selection. *J Cell Biol.* **136**:111-23.

Yang HC, Pon LA (2002) Actin cable dynamics in budding yeast. *Proc Natl Acad Sci U S A.* **99**:751-6.

Zhang G, Fedyunin I, Miekley O, Valleriani A, Moura A, Ignatova Z (2010) Global and local depletion of ternary complex limits translational elongation. *Nucleic Acids Res.* **38**:4778-87.

Zhang S, Guo Y, Boulianne G (2001) Identification of a novel family of putative methyltransferases that interact with human and Drosophila presenilins. *Gene* **280**:135-44.

Zhu W, Cowie A, Wasfy GW, Penn LZ, Leber B, Andrews DW (1996) Bcl-2 mutants with restricted subcellular location reveal spatially distinct pathways for apoptosis in different cell types. *EMBO J.* **15**:4130-41.

Zipor G, Haim-Vilmovsky L, Gelin-Licht R, Gadir N, Brocard C, Gerst JE (2009) Localization of mRNAs coding for peroxisomal proteins in the yeast, Saccharomyces cerevisiae. *Proc Natl Acad Sci U S A.* **106**:19848-53.

Figure Legends

Figure 1:

ABP140 mRNA localizes to the distal pole of the mother cell. (**A**) Cells were grown to logarithmic phase, fixed, and subjected to FISH against ABP140 mRNA. Anti-sense probes towards different regions of the mRNA show similar staining. Only background staining was detected in a strain deleted for *ABP140*. (**B**) Quantitation of (A). Only budded cells were counted, and only those cells where mother/daughter pairs could be unambiguously assigned in the DIC channel were considered. All cells where the brightest signal was close to the cortex in an area spanning 60° to both sides of the central axis, either dot- or crescent-shaped, were considered positive. For every condition, a minimum of one hundred cells from at least two independent experiments was counted. Error bars designate the 95.4% confidence interval or two standard deviations. The confidence interval was determined assuming random sampling and using the normal approximation for a binomial distribution. *** denotes statistical significance with $P < 0.001$ in a one-tailed two proportion z-test. The c in superscript indicates that *Δtpm1* was compared to an untreated wild-type sample for statistical testing. (**C**) ABP140 mRNA localization is dependent on actin. FISH against ABP140 mRNA in a *Δtpm1* mutant, which has no detectable actin cables. Alternatively, cells were treated with 30 μg/ml latrunculin A, which prevents polymerization of actin cables, for 10 min. Treatment with 30 μg/ml benomyl for 15 min could not phenocopy the effect of latrunculin A on ABP140 mRNA localization. (**D**) Quantitation of (C). See (B) for details. The white bars in (A) and (C) correspond to 5 μm.

Figure 2:

ABP140 mRNA localizes to the end of actin cables, independently of 3' and 5'UTR. (**A**) 5' and 3' UTR are not required for localization of ABP140 mRNA to the distal pole. FISH against ABP140 mRNA in strains where either 5' UTR, 3' UTR, or both, were exchanged for the corresponding sequences from the *ADH1* locus. The mRNA was detected at the distal pole in all cases. Exposure times for pADH1 constructs were reduced to compensate for the increase in signal strength. (**B**) Quantitation of (A). See Fig. 1B for details. The three UTR-constructs showed no significant decrease in localization if compared to the wild-type in a one-tailed two proportion z-test. Sketches of the constructs are included: Gray represents endogenous sequences, while white parts are taken from exogenous sources. The wider area corresponds to the ORF. Additional features of the protein are indicated: N17: actin-binding domain; RNA: putative RNA-binding domain; RFS: ribosomal frameshift site. (**C**) Confocal microscopy on FISH/IF against ABP140 mRNA and GFP in cells expressing Abp140-GFP under an ADH1 promoter. ABP140 mRNA signal frequently colocalized with actin cables (72% of 356 foci counted). The white bars in (A) and (C) correspond to 5 μm.

Figure 3:

Localization of Abp140p determines localization of ABP140 mRNA. (**A**) Live-cell imaging of GFP fluorescence or FISH against ABP140 mRNA in various strains expressing different GFP-tagged constructs of *ABP140*. Exposure times for pADH constructs were reduced to compensate for the increase in signal strength. (**B-D**) Abp140p is required for ABP140 mRNA localization. (**B**) FISH against ABP140 mRNA in a strain expressing GFP-TAA-ABP140 which harbors an in-frame stop codon after the N-terminal GFP. In the absence of Abp140p, ABP140 mRNA signal dispersed. (**C** and **D**) Construct GFP-TAA-ABP140 is expressed. (**C**) Western blot for GFP on total lysate. 30 μg of total protein were analyzed. (**D**) Quantitative RT-PCR with primers specific for *ABP140*. *PGK1* was used to normalize the samples. Endogenous *ABP140* was set to 1.0. GFP-TAA-ABP140 mRNA is present in similar

amounts as the wild-type transcript when placed under the same promoter (pADH1) (**E**) Quantitation of (A) and (B). Sketches of the constructs are included. See Fig. 1B and 2B for details on the representation. The white bars in (A) and (B) correspond to 5 μm.

Figure 4:

The first 67 amino acids of Abp140p are sufficient to localize the mRNA to the distal pole. (**A**) Western blot against GFP on total lysates generated from strains expressing different GFP-tagged C-terminal truncations of *ABP140*. (**B**) FISH against GFP on the truncations shown in (A). The first 67 amino acids are sufficient to localize the mRNA to the distal pole when fused to GFP. The white bar corresponds to 5 μm. (**C**) Quantitation of (B). Sketches of the constructs are included. See Fig. 1B and 2B for details on the representation.

Figure 5:

Localization of ABP140 mRNA is dependent on the length of the ORF. (**A**) Amino acids 18-67 are not specifically required for mRNA localization. FISH against ABP140 mRNA in cells where amino acids 18-67 of *ABP140* were replaced by GFP. In the control strain, GFP is inserted between amino acids 17 and 18. ABP140 mRNA localization to the distal pole is not affected in these strains. (**B**) FISH against GFP in cells expressing (1-17)-GFP, (1-17)-4GFP, (1-67)-GFP, or (1-67)TAA-GFP. The exposure time for the quadruple GFP construct was reduced to compensate for the increase in signal strength. If the actin-binding domain is appended with four copies of GFP instead of one, mRNA localization to the distal pole is recovered. If a stop codon is inserted between ABP140(1-67) and GFP, mRNA localization to the distal pole is lost. (**C**) Quantitation of (A) and (B). Sketches of the constructs are included. See Fig. 1B and 2B for details on the representation. The white bars in (A) and (B) correspond to 5 μm.

Figure 6:

Active translation is required for ABP140 mRNA localization to the distal pole. (**A**) Wild-type and *prt1-1* mutant cells were shifted to 37°C for 20 min and processed for FISH against ABP140 mRNA. In the translation initiation mutant, localization of ABP140 mRNA to the distal pole was greatly reduced. (**B** and **C**) Polysome profile analysis on yeast lysates. The positions of the 80S peak and the polysome fraction are indicated. Translation was blocked either in a conditional translation initiation-deficient mutant that was shifted to the non-permissive temperature (37°C) for 20 min (B) or by treatment of wild-type cells with 10 μg/ml Verrucarin A for 1 h (C). The control was incubated with the solvent. (**D** and **E**) FISH against ABP140 mRNA on wild-type cells (D) or on yeast expressing ABP140-3'ASH (E) that were treated with either 10 μg/ml Verrucarin A for 1 h, or 100 μg/ml CHX for 20 min. Control cells correspond to the chloroform control for Verrucarin A treatment. (**F**) Abp140p is not depleted during Verrucarin A treatment. Western blot against GFP on total lysate of cells expressing Abp140-GFP that were treated with 10 μg/ml Verrucarin A for 1 h. Per lane, 30 μg of total protein were loaded. (**G**) Quantitation of (D) and (E). Sketches of the constructs are included. See Fig. 1B and 2B for details on the representation. The white bars in (A), (D) and (E) correspond to 5 μm.

Figure 7:

Live-cell imaging of ABP140 mRNA dynamics. (**A**) Live-cell imaging of GFP fluorescence in cells expressing pADH-ABP140-MS2/MS2-GFP or pADH-ABP140-U1A/U1A-GFP. Sketches of the constructs are included. See Fig. 2B for details on the representation. (**B**) Time-lapse imaging of an ABP140-MS2/MS2-GFP particle moving towards the distal pole. The images correspond to a subarea of a movie that can be viewed in full in the

supplementary material (Suppl. Movie 3). (**C**) Particle trace of (B). Each color represents a different 10s time point. Particles that moved between two consecutive frames are connected with white lines (dt = 10s). (**D**) Particle trace of Suppl. Movie 4 as in (C). Stills can be found in Suppl. Fig. 6. (**E**) Time-lapse imaging of an ABP140-MS2/MS2-GFP comigrating with a brighter patch on an actin cable marked by (1-17)Abp140p-2xmCherry. The full movie can be viewed in the supplementary material (Suppl. Movie 6). The white bars in (A), (C), (D), and (E) correspond to 5 μm.

Figure 8:

Model of the cotranslational transport of ABP140 mRNA to the distal pole. In the course of translation, the N-terminal actin-binding domain of Abp140p is exposed to the cytoplasm and binds actin cables. The complex of nascent protein, ribosome, and mRNA is transported to the distal pole by actin retrograde flow. The bulk of the protein would then be generated at the distal pole and distributed from there.

Kilchert et al., Figure 1

A

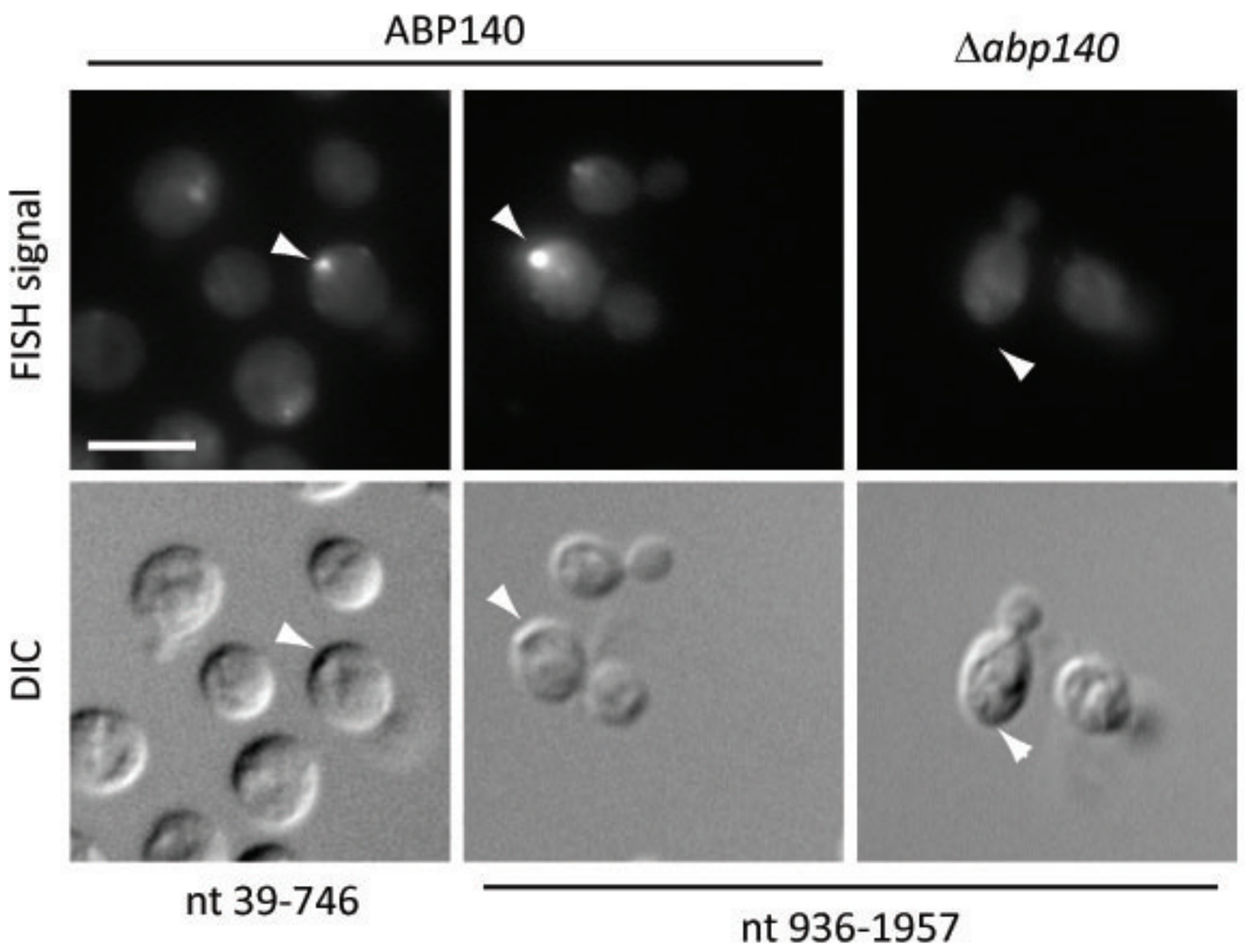

B

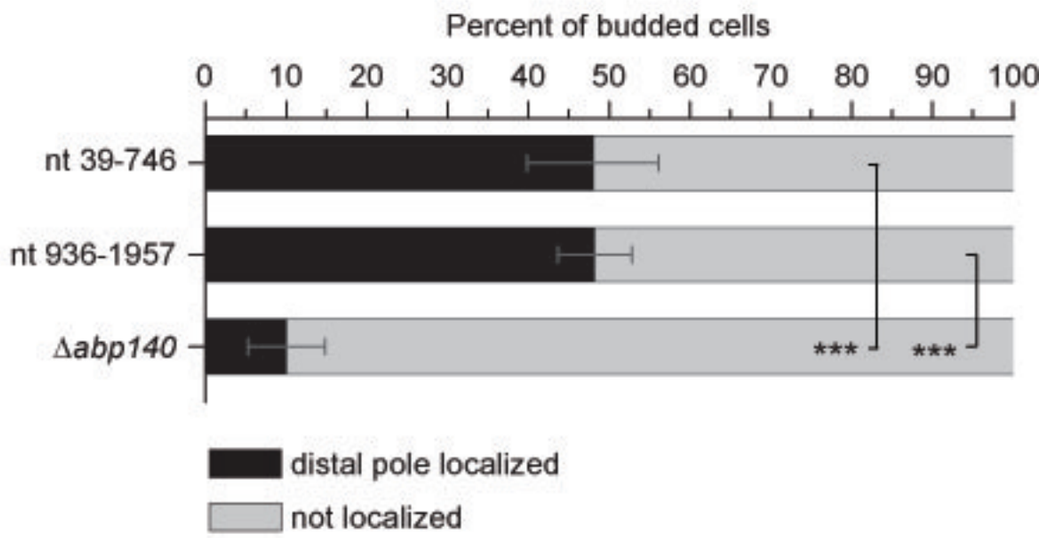

C

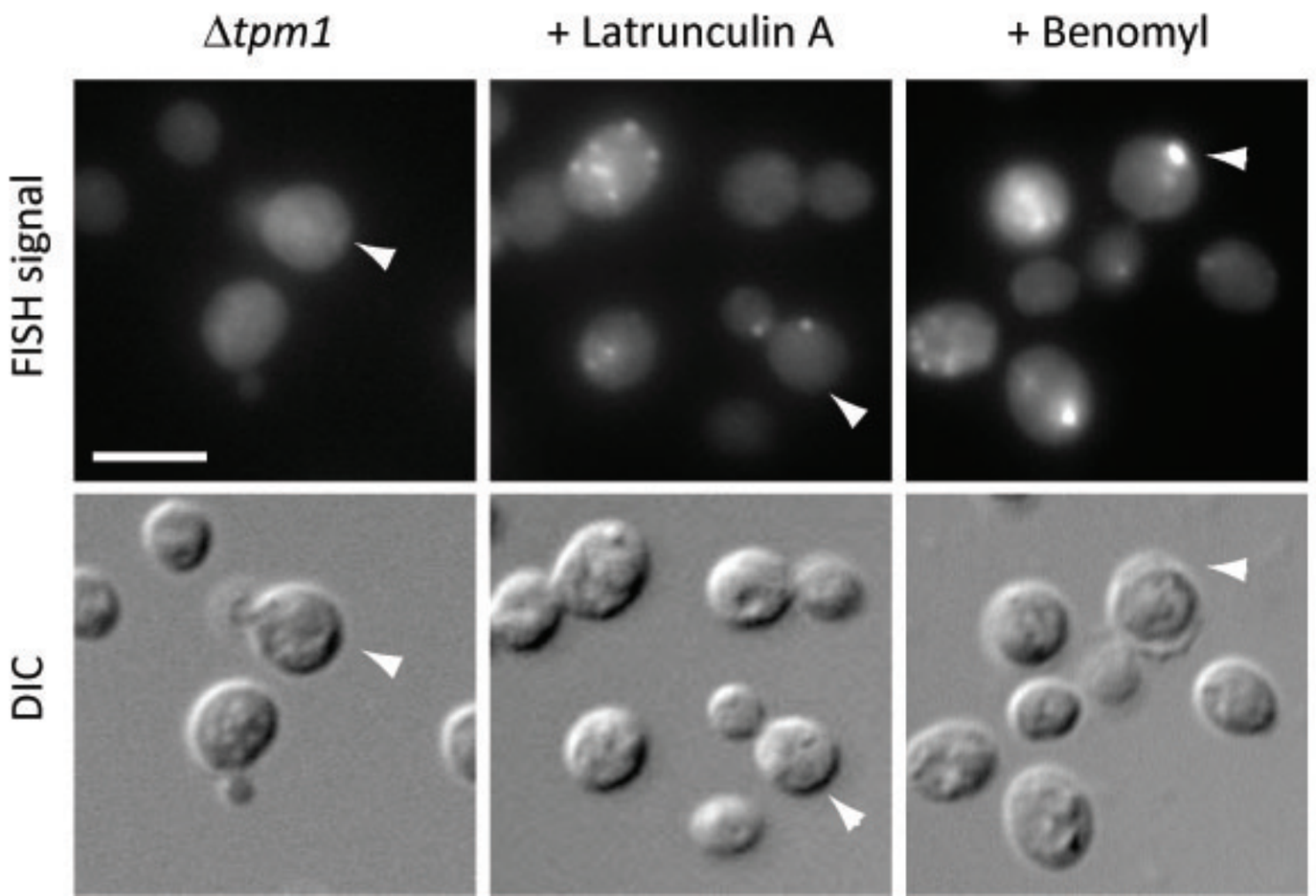

D

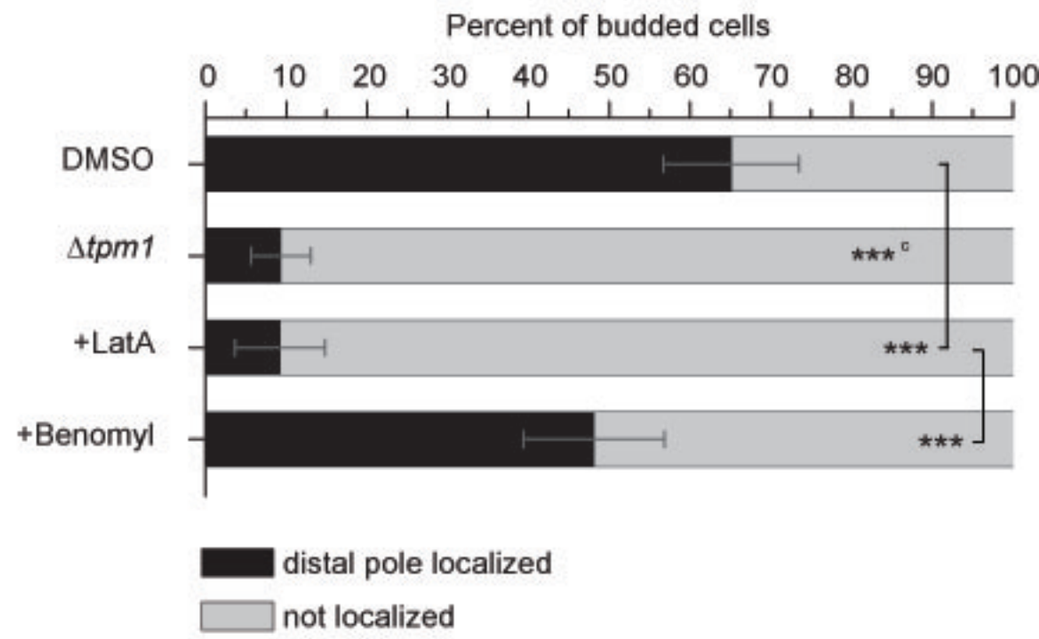

Kilchert et al., Figure 2

A

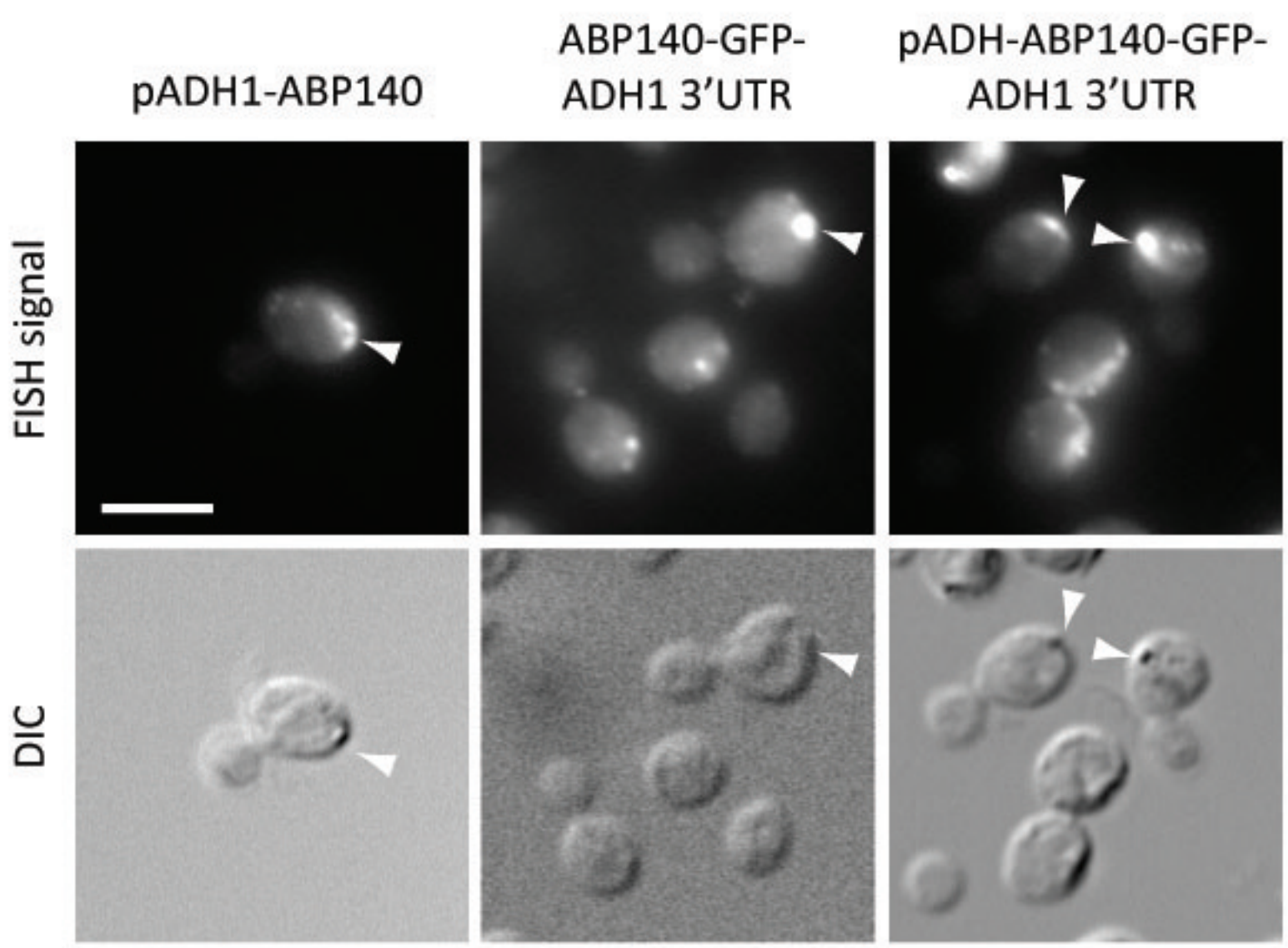

B

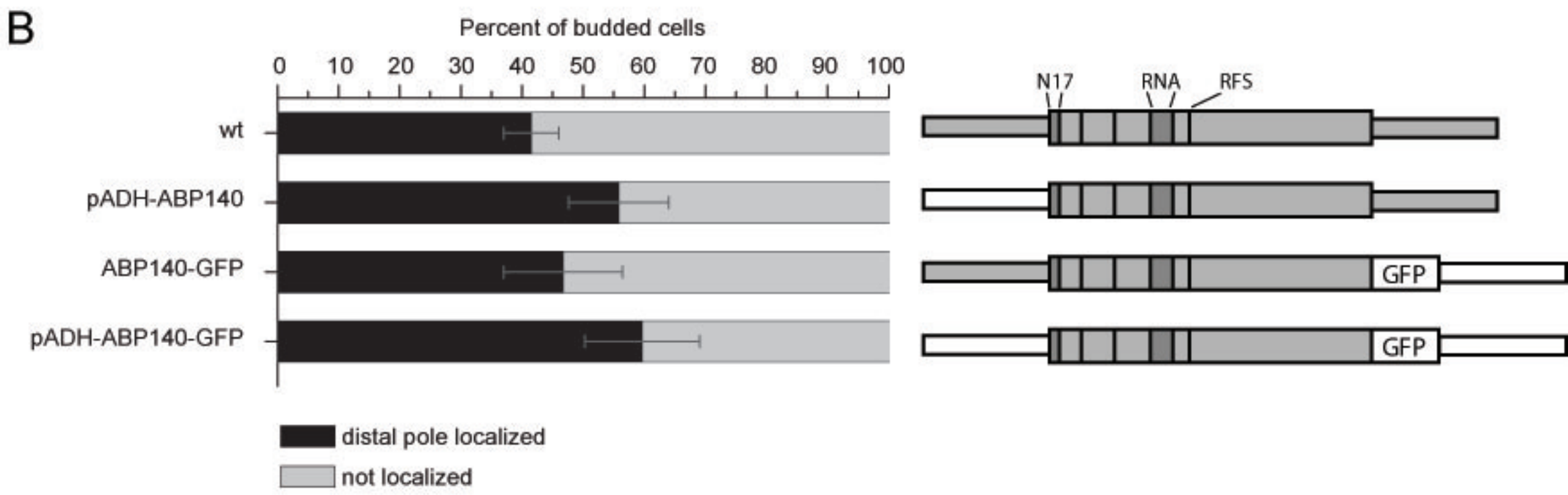

C

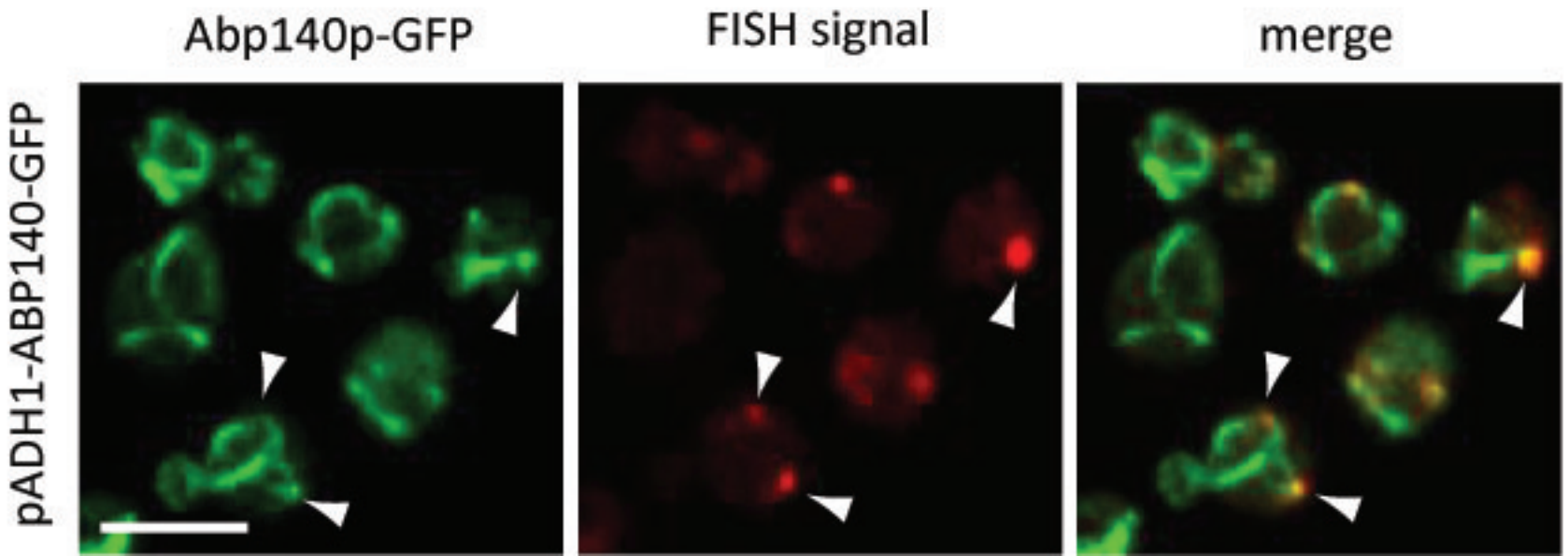

Kilchert et al., Figure 3

A

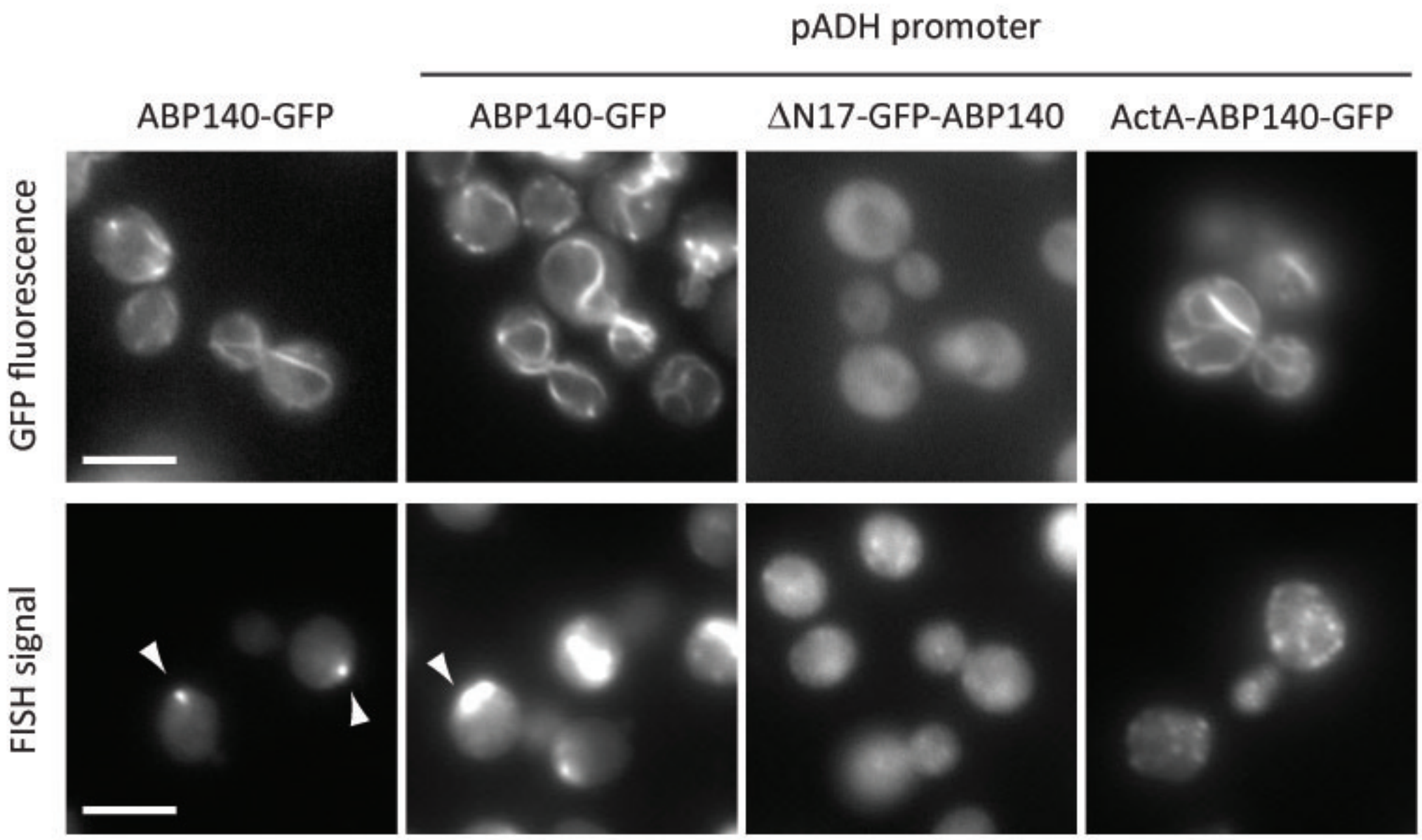

B

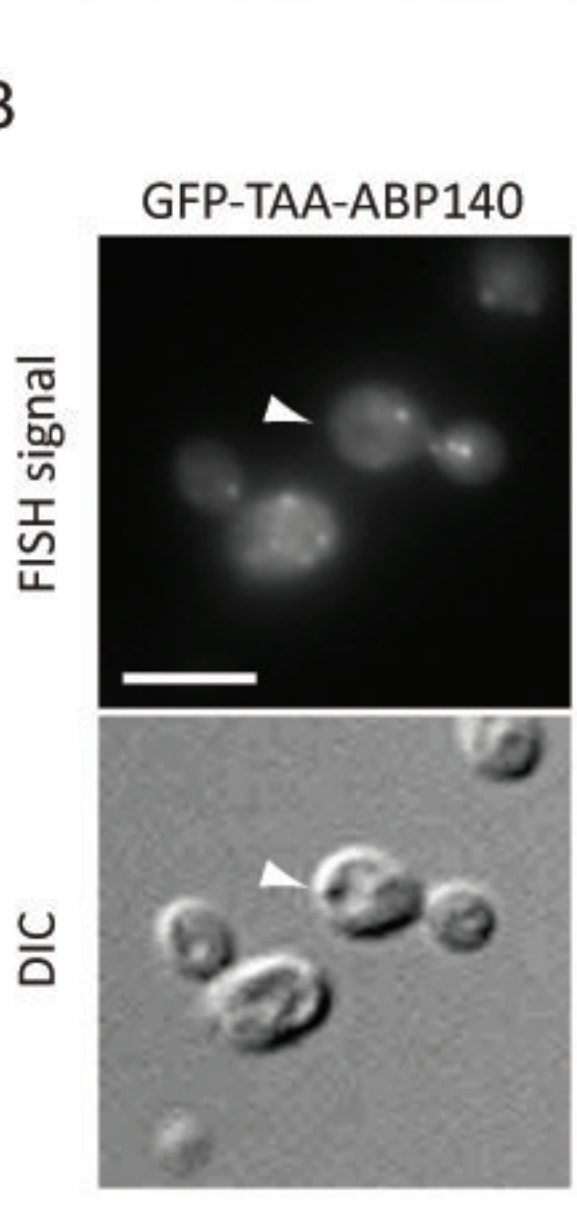

C

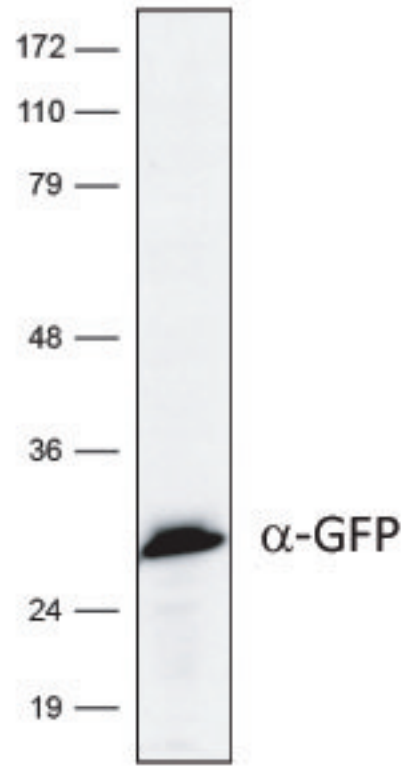

D

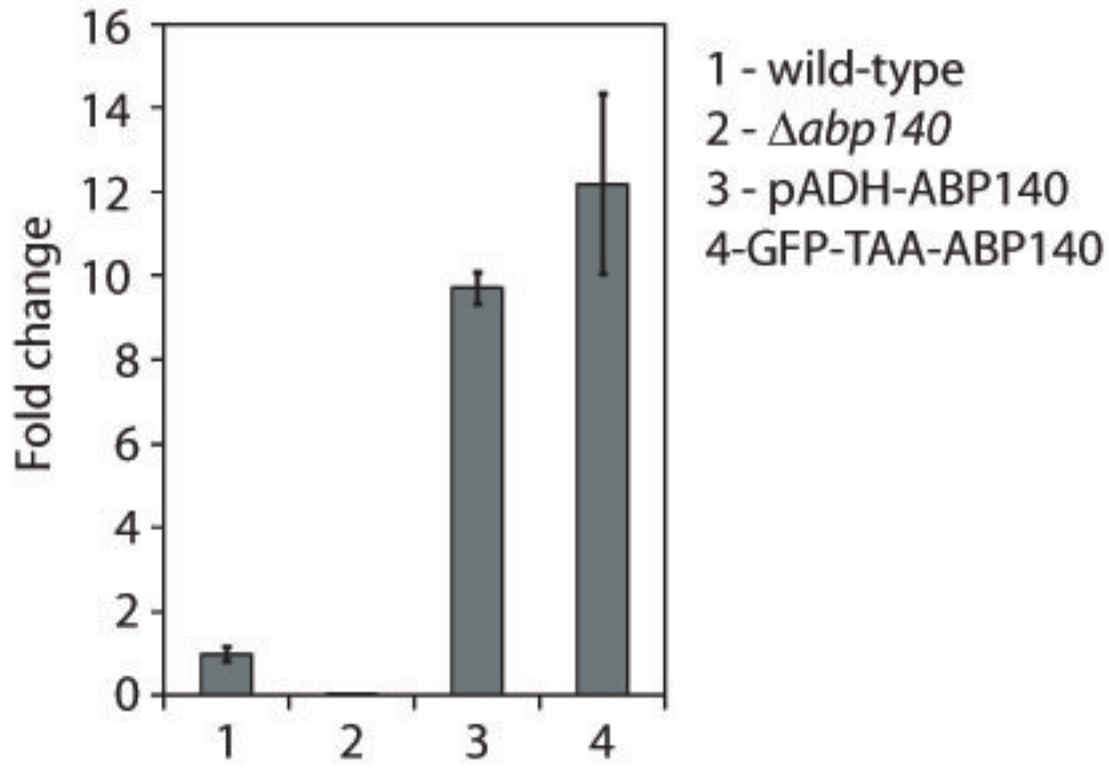

E

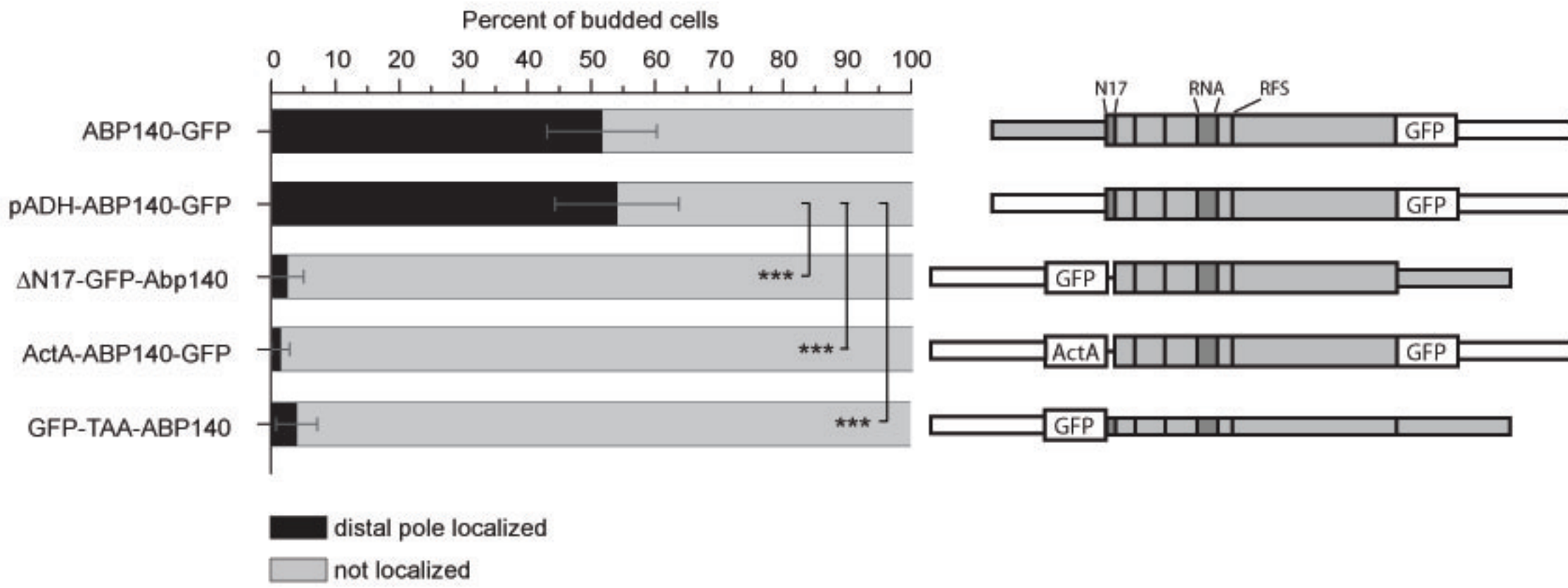

Kilchert et al., Figure 4

A

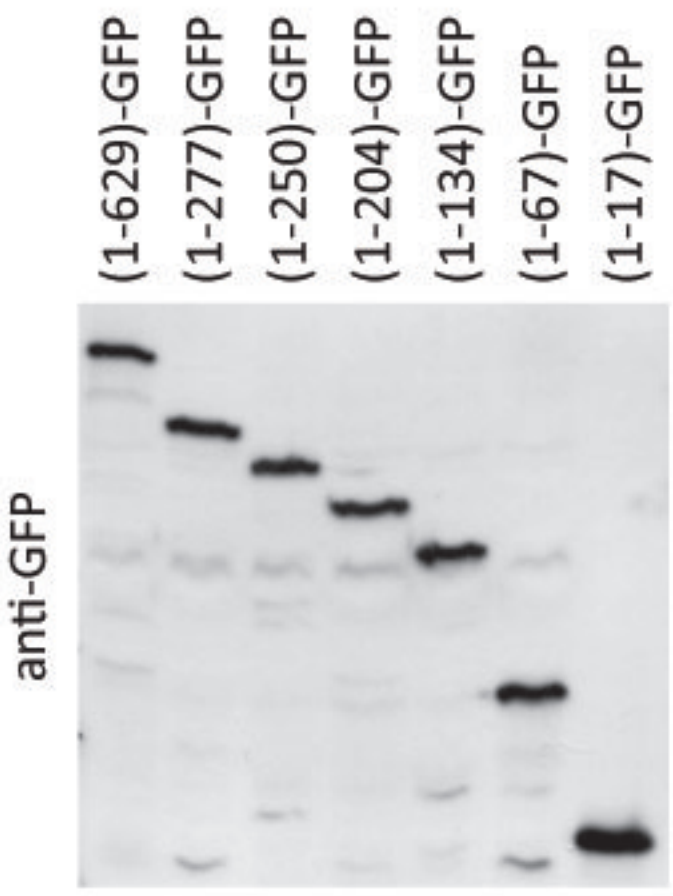

B

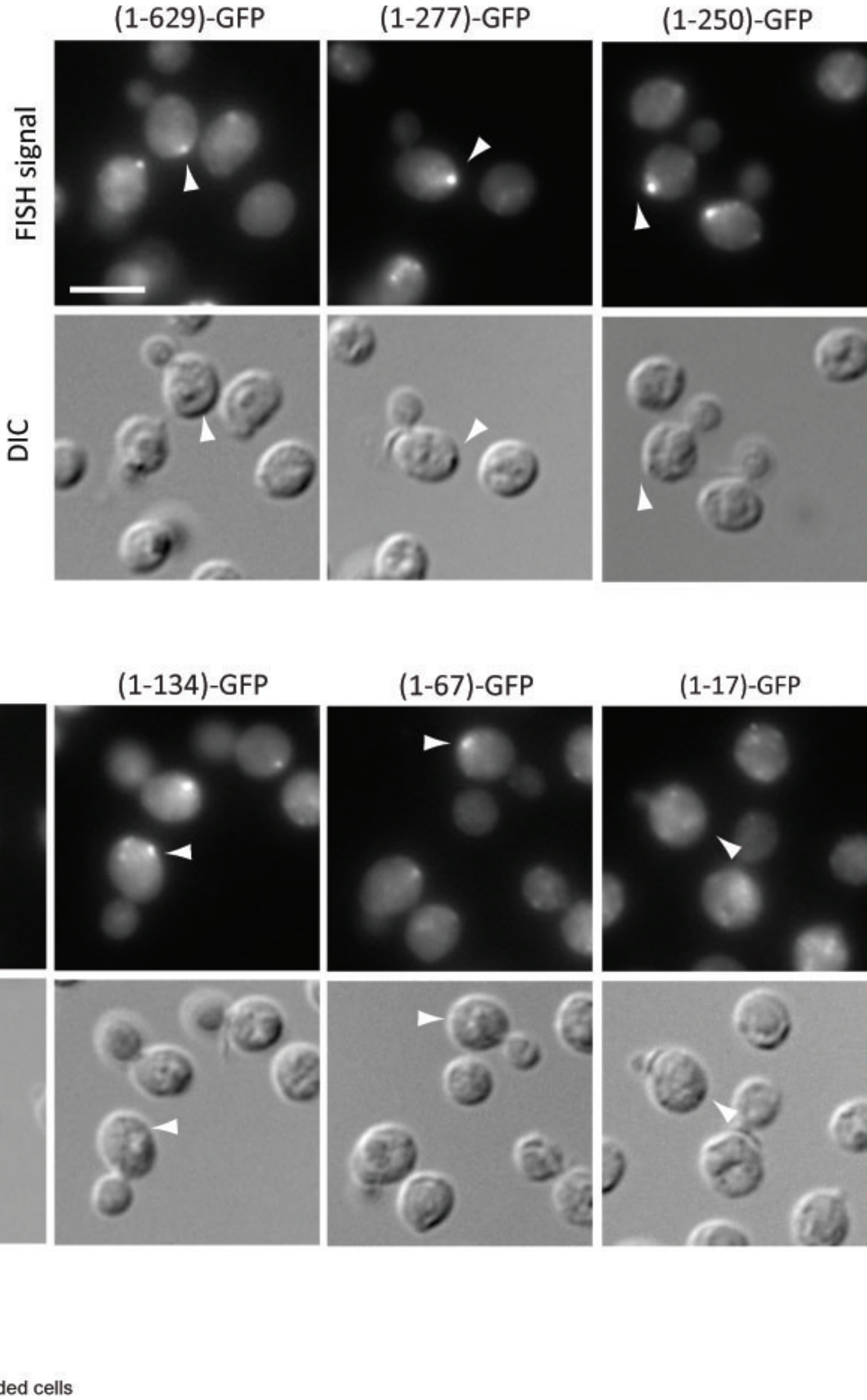

C

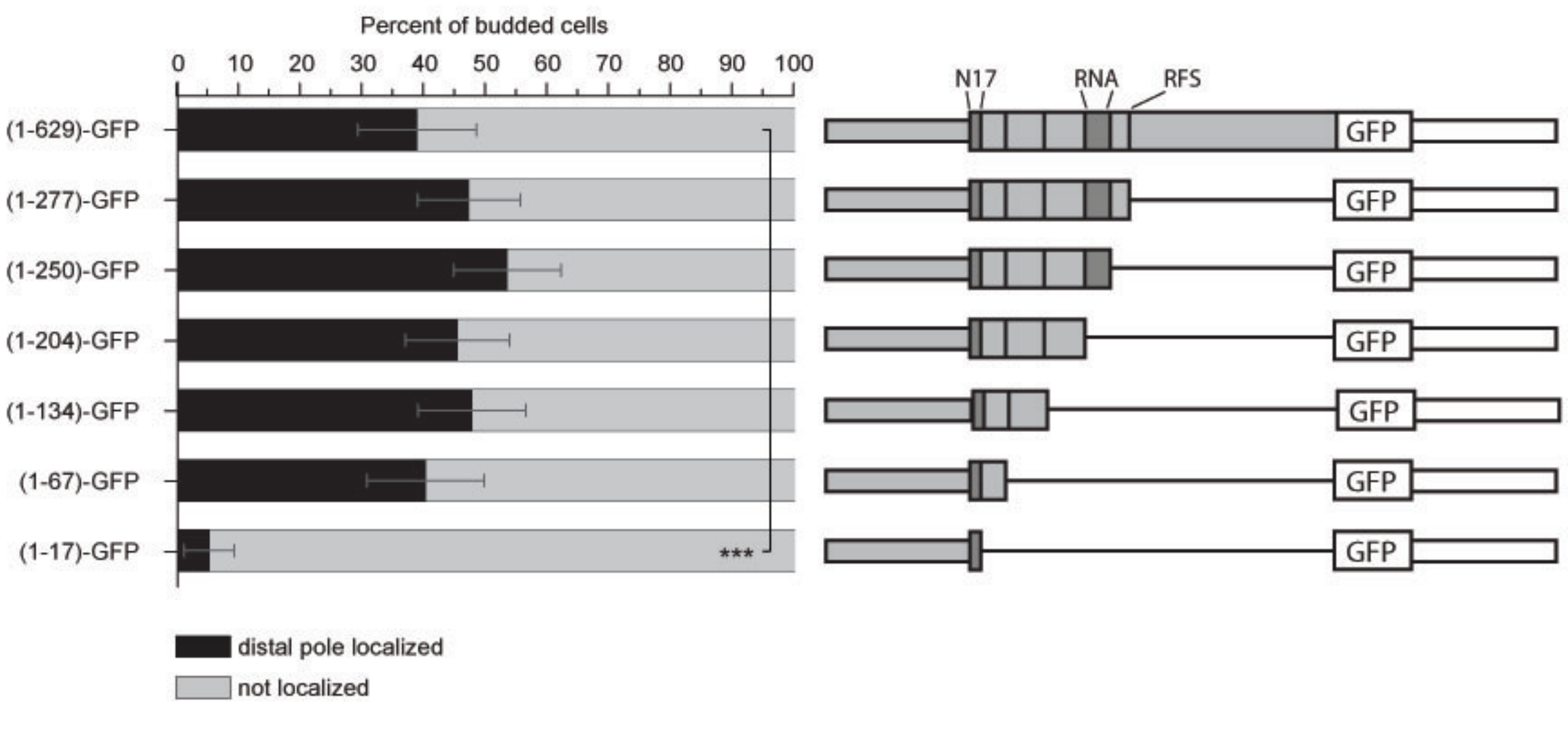

Kilchert et al. , Figure 5

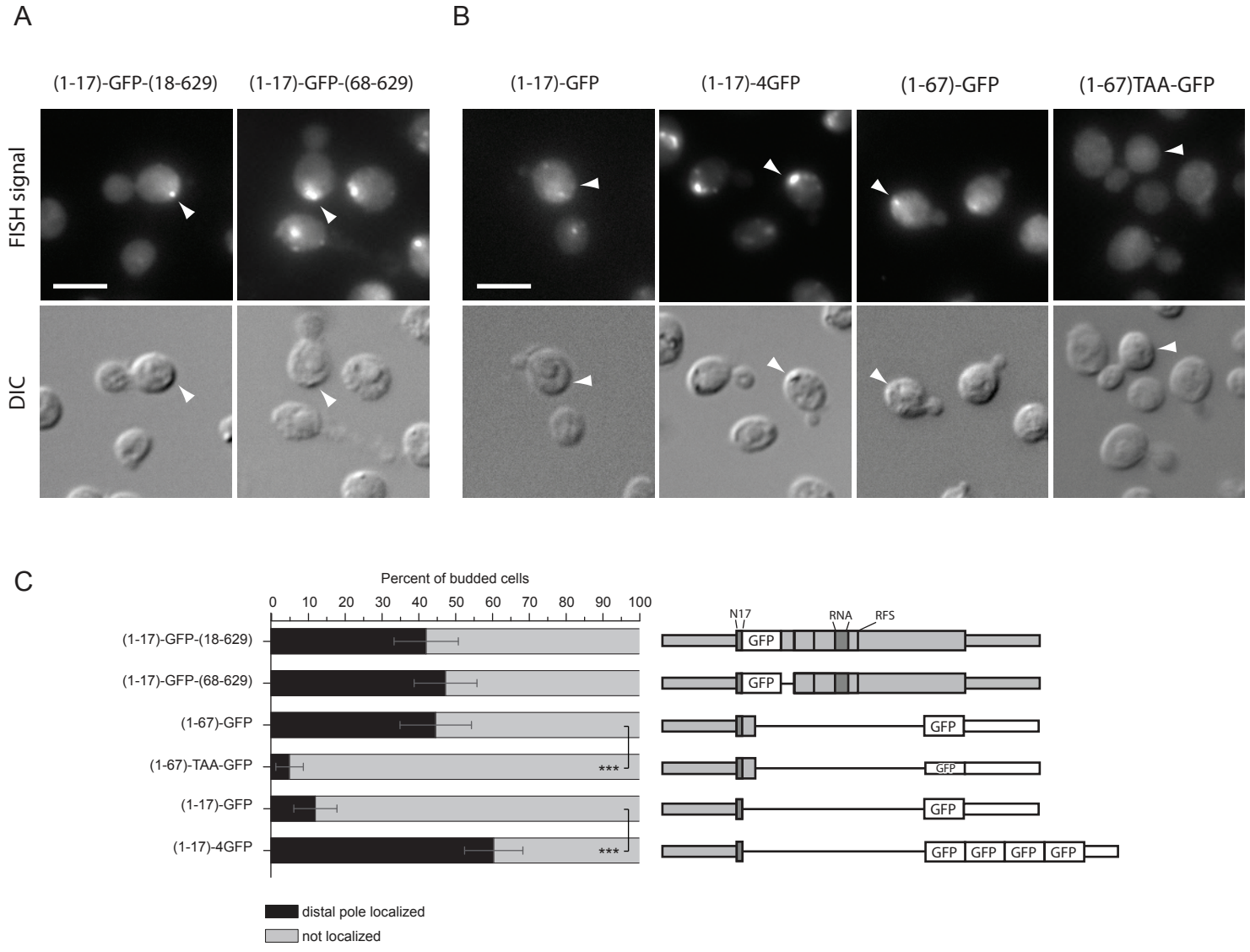

Kilchert et al., Figure 6

A

FISH signal

DIC

23°C 37°C

prt1-1

B

polysomes

80S

23°C 37°C

prt1-1

C

control + Verrucarin A

wild-type

D

FISH signal

DIC

control + Verrucarin A +CHX

wild-type

E

control + Verrucarin A +CHX

ABP140-3'ASH

F

ABP140-GFP

Verrucarin A - +

anti-GFP

G

Percent of budded cells

0 10 20 30 40 50 60 70 80 90 100

wild-type

wild-type + V A

wild-type + CHX

3'ASH

3'ASH + V A

3'ASH + CHX

***

***

distal pole localized

distal pole and bud-tip

not localized

bud-tip localized

Kilchert et al., Figure 7

A

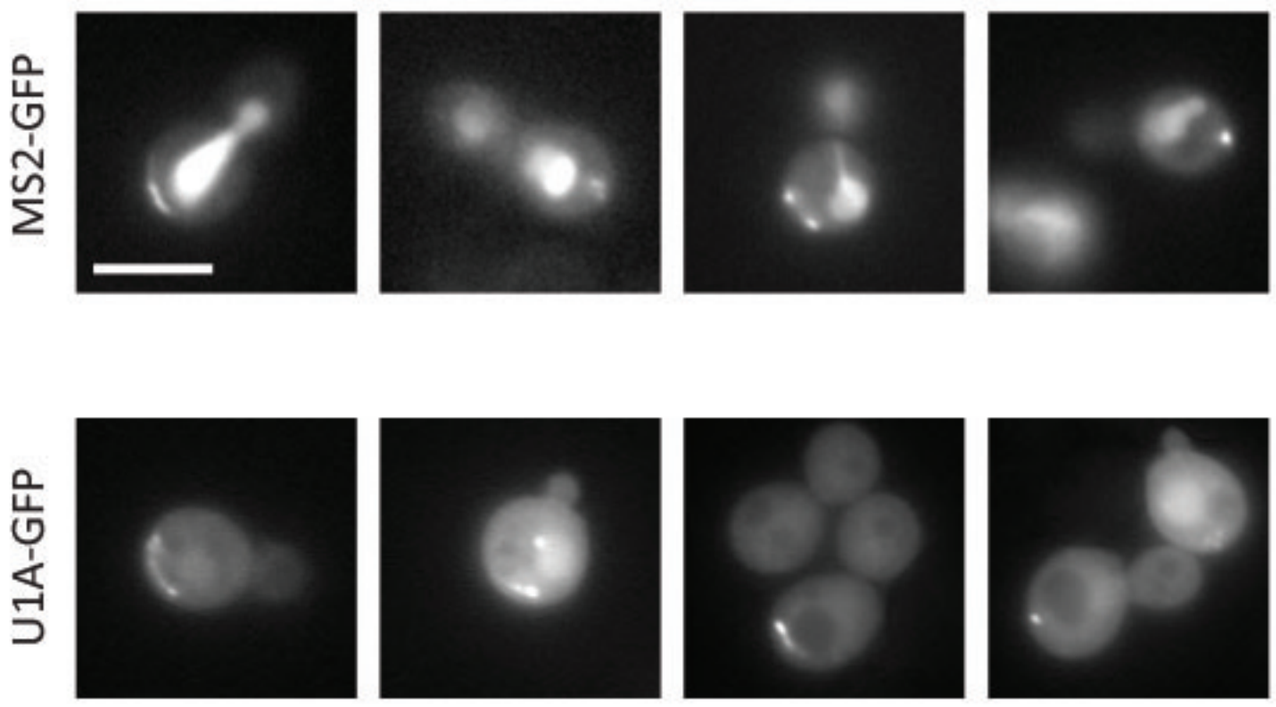

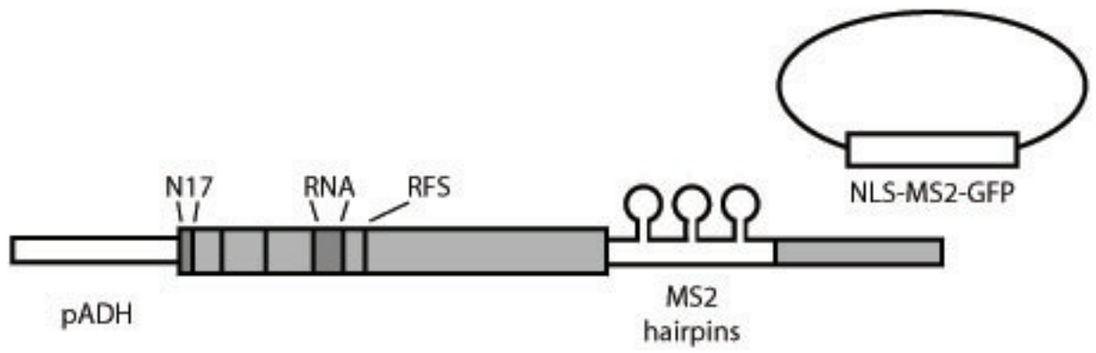

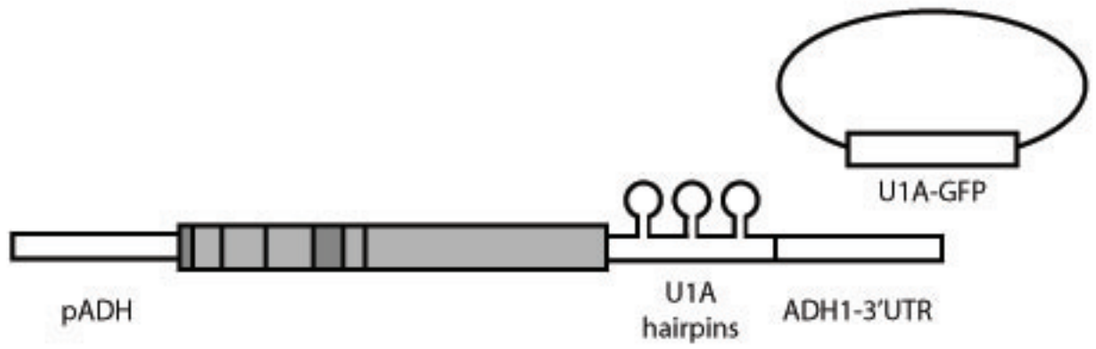

B

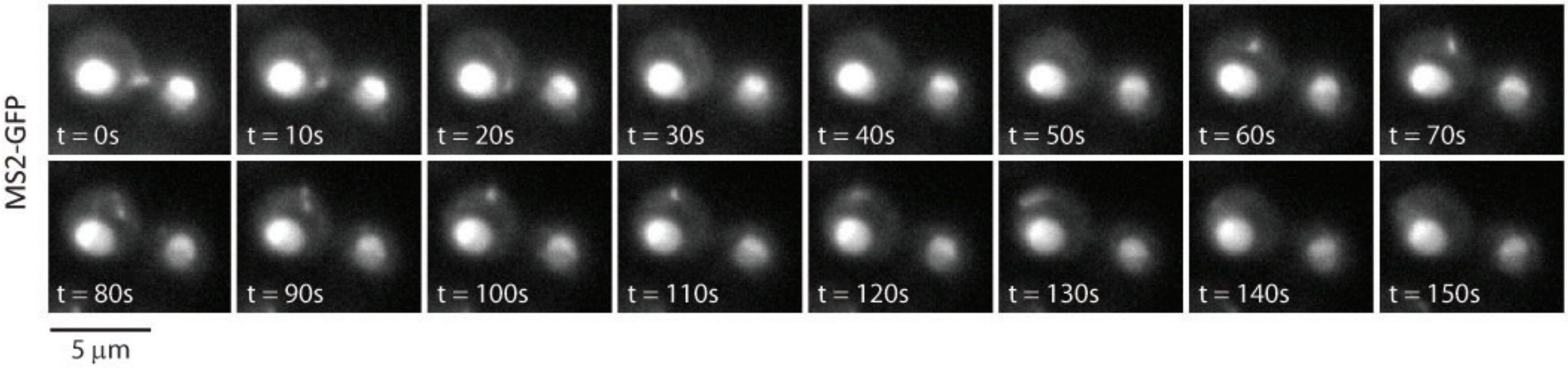

C

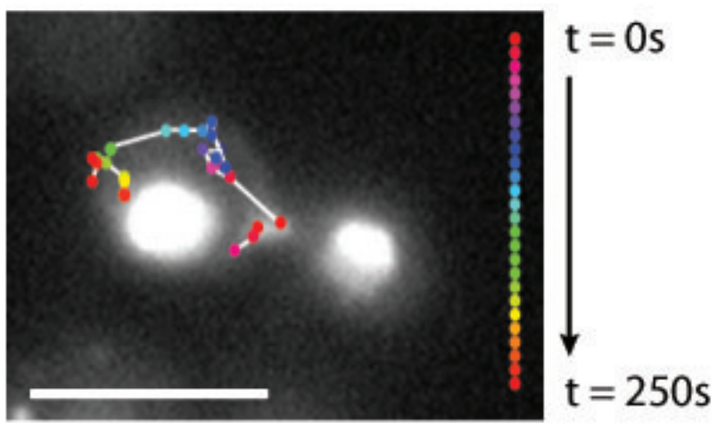

D

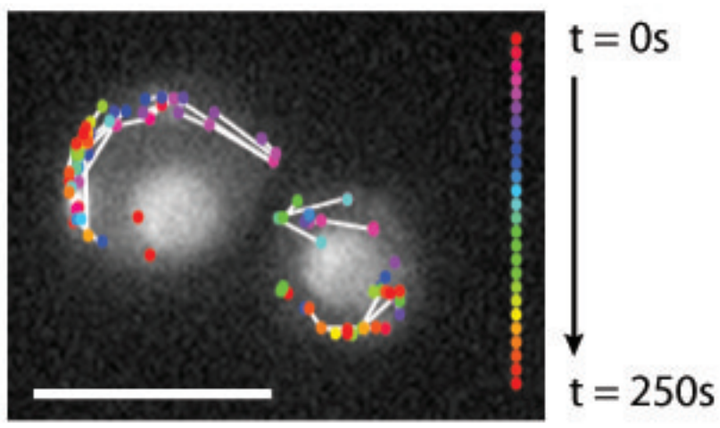

E

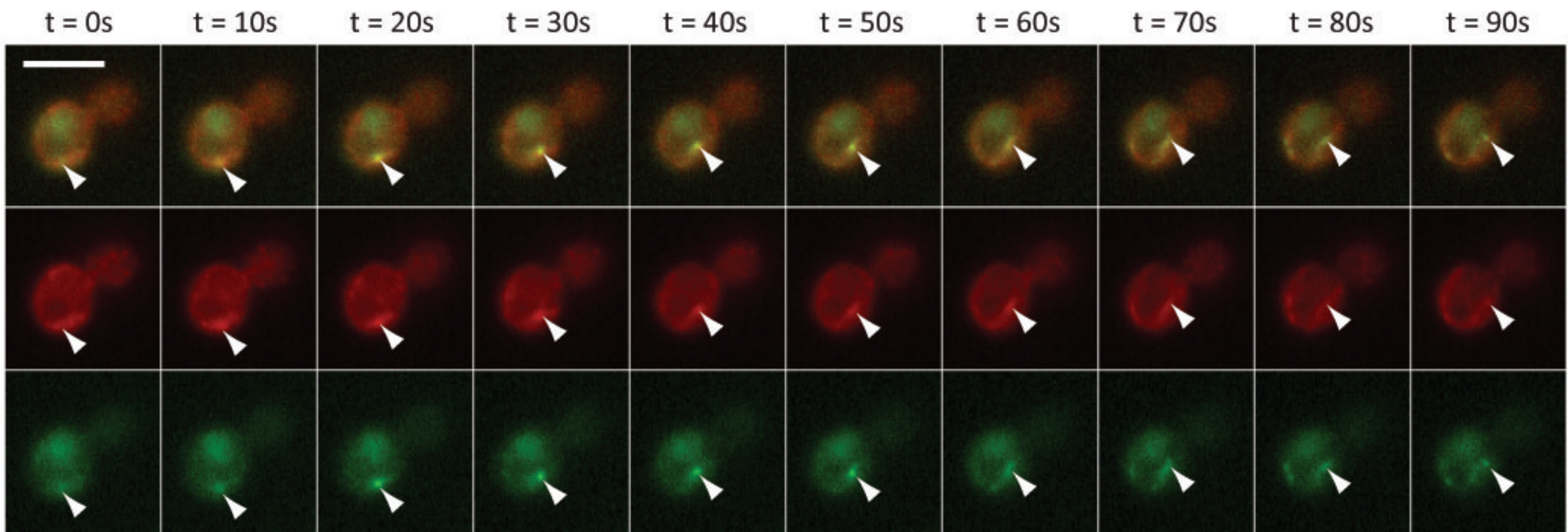

Kilchert et al., Figure 8